5

FGFs and other molecules that differentially govern the process of EMT in healing tail and limb

The previous chapter emphasized on the wound healing process wherein the wound epithelium is successfully achieved in tail and scarring begins in the limb following amputation. The current chapter focusses on what happens after the wound epithelium is achieved in the tail and what changes occur, succeeding to the scar formation in the limb.

INTRODUCTION

In terms of regeneration, lizards are the closest organisms to mammals which can replace an entire appendage (autotomised tail) and yet somehow is one of the least studied model organisms for regeneration (Lozito and Tuan, 2017). Most studies in regeneration are biased towards zebrafish and salamanders, and hence studying the mechanism behind lizard's tail regeneration is of paramount significance in order to fill the void. Zebrafish and salamanders can regenerate most of their organs and therefore are preferred models for study (Tanaka, 2003; Poss, 2007; Chávez et al., 2016; Sehring et al., 2016). However, unlike salamanders, lizards cannot regenerate their limbs, and consequently, they make an exceptional candidate to study scar-free wound healing in tail and scarring (which resembles mammalian wound healing) in limb (Bryant and Bellairs, 1977; Alibardi, 2009, 2018; Miller et al., 2019). The exact reason for this differential healing in tail and limb is yet to be unfolded.

However, in order to decipher the mechanism through which scar-free and scarred wound healing are regulated, understanding the processes and their pattern at different time points is deemed necessary. There are many processes which govern the healing pattern for scar-free and scarred wound healing, like, haemostasis, inflammation, and wound closure by epithelium (Barrientos et al., 2008). These are the conventional processes shared between both the healing types. However, the duration of these processes succeeding injury are different prior to re-epithelialization as seen in lizard *Hemidactylus flaviviridis* (Ranadive et al., 2018). Apart from these processes mentioned above, there are other events in scar-free wound healing, which lead to the formation of multi-layered wound epithelium that trigger the regenerative response in a regeneration enabled appendage.

The wound epithelium mentioned above is characterised by a stratified layer of epithelia also known as an apical epithelial cap (AEC) and is the first main stage of epimorphic regeneration (Bernet et al., 2018; Brito, 2018). It is but logical to perceive that, replacing an amputated structure, in most of the regenerating organisms, requires continuous supply of cells. Hence, as soon as AEC is formed it acts as an organizer to direct the cells immediately beneath to undergo repeated mitosis and repatterning until the lost structure is rebuilt (Christensen and Tassava, 2000; Satoh et al., 2012; Stocum, 2019). Interestingly, new cells are recruited to the site of injury and proliferate to give rise to a mass of undifferentiated cells known as "blastema" (Patel et al., 2019; Tsai, 2019). This blastema is formed by either de-differentiation of the existing cells or by the proliferation of a resident stem cell population (Murawala et al., 2018). However, even though rarely, proliferation of terminally differentiated cells too contributes for the success of regeneration (Tsai, 2019). But the extent to which each of this mode is used depends on the species or even in the same species it is attributed to the type of tissue undergoing regeneration and hence, cannot be generalized. Adult stem cells are present in many of the vertebrate tissues which have a crucial role in maintaining tissue homeostasis (Simmons and Clevers, 2011). However, these modes of cell supply like division, dedifferentiation, and transdifferentiation are very context dependent. A classic example is of liver, wherein if it is in extremely damaged state or in chronically infected condition, then the source of new cells is the liver progenitor cells whereas if the liver is partially damaged or cut, the regeneration is primarily achieved by proliferation of the remaining hepatocytes (Riehle et al., 2011). Another example is of zebrafish heart in which when lineage tracking was done, the results indicated that the existing cardiomyocytes undergo dedifferentiation and proliferate to generate new cardiomyocytes in order to replace and compensate the lost heart tissue (Jopling et al., 2010; Kikuchi et al., 2010). One more interesting example of dedifferentiation is during the appendage regeneration in Urodele amphibians, i.e., in newts and axolotls. In this case, after amputation of the limb, at the site of injury syncytial skeletal myotubes undergo cellularisation to produce mononucleated cells. These mononucleated cells then re-enter the cell cycle and proliferate, adding cells to the blastemal mass (Echeverri et al., 2001; Kumar et al., 2004). Additionally, satellite cells present in the skeletal muscle of adult newts also get activated and contribute to the making new tissue during regeneration. Although both the above mentioned mechanisms are seen during axolotl limb regeneration, how much is their individual contribution to the formation of blastema remains to be answered (Morrison et al., 2006). Larval tail regeneration, however, seems to be driven mostly by progenitor cells. This was substantiated by lineage

tracking experiments where the re-growth was directly correlated to the satellite cells present in the miscle before amputating the tail (Slack et al., 2004). Lineage tracking in axolotls and *Xenopus* has helped in confirming the hypothesis that multiple cell types contribute in the formation of blastema during regeneration (Slack et al., 2004; Kragl et al., 2009). Although now we know that multiple cells types are involved in blastema formation, what remains unclear is whether the cells come from progenitors cells or by dedifferentiation of mature cells.

However, a third type of mechanism, which leads to the addition of cells in the blastemal pool is now being accepted known as epithelial to mesenchymal transition (EMT) (Alibardi, 2012; Abnave et al., 2017). At present, it is a well-known fact that all the cells in our body arise from a single cell and the phenotypic variants in these different cells are because of specific expression of defined genes which further gives a functional diversity. Epithelial cells at the time of embryogenesis are thought to be plastic in nature, meaning they can switch back and forth between epithelia and mesenchyme via the process of EMT and MET (mesenchymal to epithelial transition) respectively (Theiry, 2002; Diepenbruck and Christofori, 2016; He et al., 2018). EMT is seen during three different events with diverse functional consequences, as represented in Figure 5.1. Type 1 EMT is observed during embryogenesis starting from implantation till organ development (Kalluri, 2009; Kalluri and Weinberg, 2009; Zeisberg and Neilson, 2009). Interestingly, fibrosis or uncontrolled systemic invasion of epithelial cells is not observed in the type 1 EMT, instead, they generate mesenchymal cells which can create new tissue with diverse function. One such example is of melanocytes that are derived from the neural crest cells via EMT, wherein the phenotype of the cells is invasive but still different from the metastatic cells involved in epithelial cell cancer which were also stimulated by the process of EMT. The difference is that these melanocytes do not invade via circulation, which is most commonly seen in the metastatic cells, which results in epithelial cancer (as reviewed by Kalluri, 2009). The first set of mesenchymal cells, also known as the primary mesenchyme come from EMT, which is very crucial during the development. Once the development progresses and the tissue starts getting specified, the epithelia again arises by the process of MET, now called as secondary epithelia as seen in case of kidney development (Ekblom, 1996; Devuyst, 2018). Ergo, in adults when EMT occurs, it is safe to say that this phenomenon ensues by reactivation of the developmental process, which may turn lethal if not controlled. In wound healing and tissue regeneration, EMT has been reported to play an important role, and it falls under type 2 EMT

(Kalluri and Weinberg, 2009; Brabletz et al., 2018). During wound healing or regeneration, EMT begins as a part of repair associated event, which generally leads to the reconstruction of the tissue following trauma or inflammatory injury. This type 2 EMT ceases, the moment tissue gets healed, and inflammation is attenuated. In epithelial cancer, the type 3 EMT is proposed to occur wherein the untransformed epithelial cells get reprogrammed genetically to aid metastasis. These changes mainly affect oncogenes and tumour suppressor genes, which collaborate with the EMT regulatory circuitry to produce outcomes far different from those reported in the other two types of EMT. The cells which are transformed by the type 3 EMT can invade via circulation which then leads to systemic manifestations of malignant cancer progression (Kalluri, 2009; Ombrato and Mallanchi, 2014; Liang et al., 2016; Smith and Bhowmick, 2016).

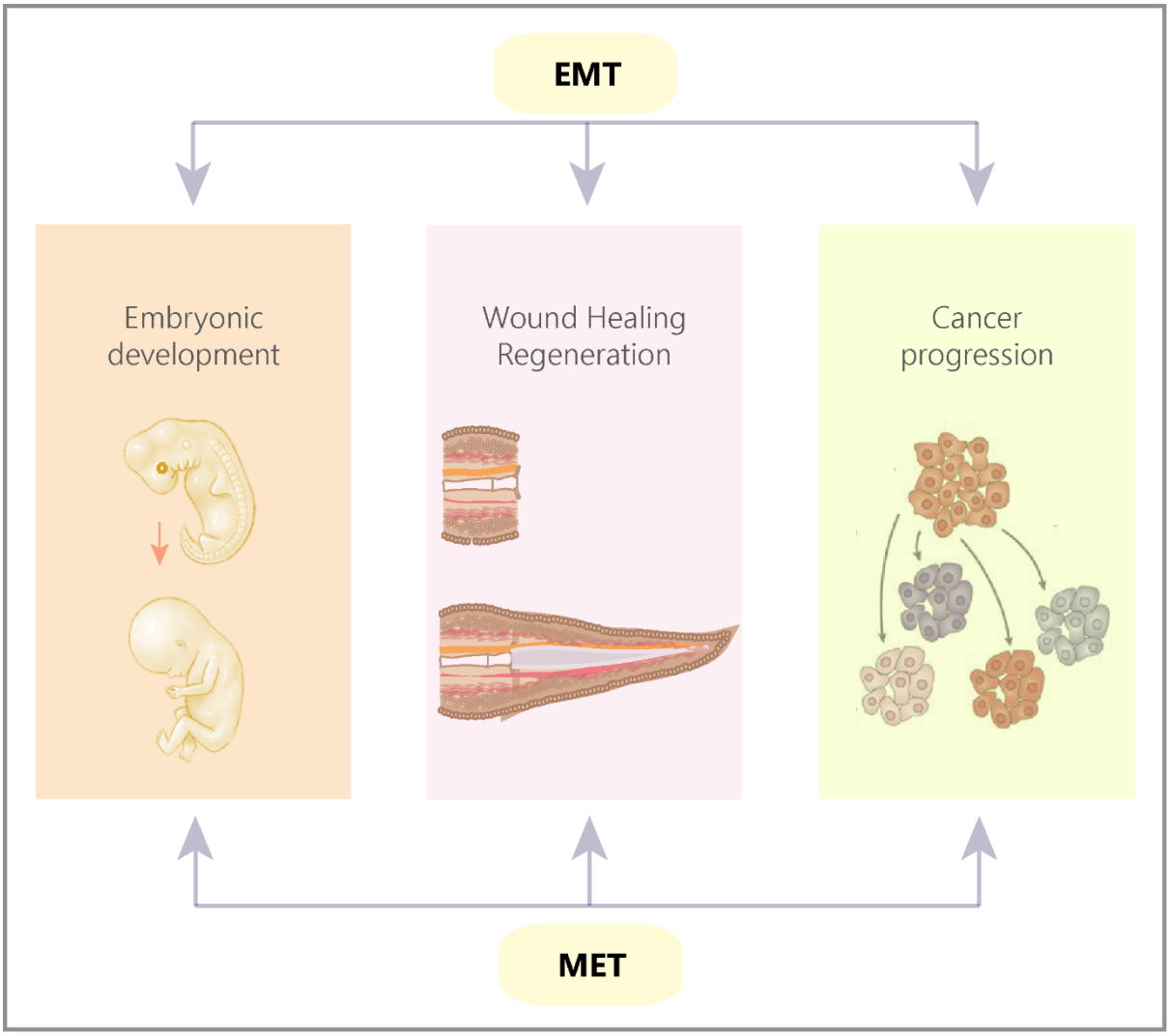

Figure 5.1: A pictorial overview of the functions of EMT and MET

It is evident from the above review that EMT should be contributing appreciably in the later phase of wound healing and regeneration, however, its role has never been validated in lizards. Moreover, as mentioned previously, the processes governing both the types of healing have similarities as well as dissimilarities, blastema being one of the latter one, which is not formed at all during the wound healing of limb. Hence, it is not far-fetched to say that the mechanisms by which blastema formation occurs in the regenerating tail are not switched on in case of the limb. The current study therefore, will focus on EMT with an aim to validate the role of EMT in the healing tail as well as limb.

MATERIALS and METHODS

Animal Maintenance:

Healthy adult northern house geckos of either sex having average snout to vent length of 10 cm were chosen for the study. They were screened for parasitic infestation, and only the healthy ones were selected for further research, while the rest were released back to their habitat. Lizards were then acclimatized for a week and maintained all through the experiment in well ventilated wooden cages. The cages were housed in a room at a controlled temperature of 36±2 °C and 40-70 % relative humidity. The photoperiod was kept at 12:12 hours of light and dark cycle. Lizards were fed with cockroach nymphs daily, and water was given *ad libitum*. Autotomy was induced in the tail by applying mild pressure with a foot ruler on the 3rd segment from the vent. The limb was amputated under hypothermia. The animal was placed on a pre-cooled tile, and ice pack was applied to the limb to be amputated. With a sharp, sterile surgical blade, the forelimb of the lizard was amputated. The experimental protocol (MSU-Z/IAEC/15-2017) was approved by the Institutional Animal Ethics Committee (IAEC), and all the experiments were performed as per the guidelines of CPCSEA (Committee for the Purpose of Control and Supervision of Experiments on Animals), India.

Experimental design

The tissue samples were harvested in a sterile condition at the selected time interval. Time points for tissue collection were decided based on the discrete events associated with wound healing and blastema formation in the tail while scarring in the limb. These have been characterized for the tail through the course of various studies in our lab (Buch et al., 2018, 2018; Murawala et al., 2018, Ranadive et al., 2018). It has been observed by both histology

and morphological profiles that the tail healing starts with the formation of epithelial covering by 2-3 dpa and AEC forms by 4 dpa followed by blastema formation at 6 dpa. Since the current study focuses on blastema formation, the following time points were used, 0 dpa (representing uncut resting stage), 1 dpa, 3 dpa, 4 dpa, and 6 dpa.

On the other hand, wound healing in the amputated limb is achieved only on 9 dpa in the selected housing condition. Based on the continuous morphological observation on an amputated limb it was noticed that the events occurring in the healing limb were quite different and it took longer to heal compared to tail. Similar observations were also made by Alibardi, (2010) and Vitulo et al., (2017). Therefore, even on 3 dpa, the cut end of limb shows only a scab with no epithelial layer beneath it. On 6 dpa, limb displays a thick blood clot and is in the granulation phase. Proper scarring is, however, achieved on 9 dpa and continues till 12 dpa after which only maturation of the scar is observed. Hence, the time points selected for limb were 0 dpa (representing uncut resting stage), 6 dpa, 9 dpa, and 12 dpa.

The study is composed of nine groups in total; five groups in case of the tail and four groups for limb tissues. Each group consisted of six lizards for individual experiments. The tissues were processed as per the requirement described in the following methodology.

Immunohistochemistry

For immunolabelling, longitudinal cryosections (8-10 μm) were cut from freshly collected tissues, fixed in acetone at -20 ºC for 15-20 min and air dried for 15 min. Sections were then rehydrated with PBST (Phosphate Buffered Saline with 0.025 % Tween-20) followed by blocking with normal serum [Genei, Merck, USA; 10 % in PBS with 0.5 % Bovine serum albumin (PBS-BSA)] for 1 hr at room temperature (RT). Sections were then incubated with Anti-N-Cadherin IgG mouse (DSHB IOWA, 0.5 μg/ml) and Anti-E-Cadherin IgG mouse (DSHB IOWA, 0.5 μg/ml). For both primary antibodies, FITC-conjugated secondary antibodies (Sigma Aldrich USA, 0.1 μg/ml) were used, and their expression was observed under a fluorescent microscope. In order to observe the proper histology of the sections, DAPI was used to counterstain them. The representative images were captured using a digital camera (Leica, EC3) mounted on the Leica DM2500 microscope. The fluorescence intensity of all IHC images was measured by ImageJ software.

Western Blot

Tissues were harvested from all the nine groups and homogenized in lysis buffer (50 mM Tris pH 7.5, 200 mM NaCl, 10 mM $CaCl_2$, and 1 % Triton-X 100) containing protease inhibitor. The samples were centrifuged at 12000rpm for 10min, and protein estimation was done using the Bradford method (Bradford, 1976). 40 µg of protein of each sample was loaded and separated on a 12% SDS-PAGE. These proteins were transferred onto PVDF membrane through semi-dry transfer method by applying 100 mA for 25 min. The primary antibodies used to probe each protein of interest were Anti-MMP9 IgG goat (Sigma-Aldrich, USA, 0.1µg/ml), Anti-MMP2 IgG goat (Sigma-Aldrich, USA, 0.1 µg/ml), Anti-N-Cadherin IgG mouse (DSHB IOWA, 0.5 µg/ml), Anti-E-Cadherin IgG mouse (DSHB IOWA, 0.5 µg/ml), Anti-Vimentin IgG mouse (DSHB IOWA, 0.5 µg/ml) and Anti-β-actin IgG mouse (Santa Cruz Biotechnology USA, 0.01µg/ml). The blots were developed by using the ALP, BCIP-NBT system (Sigma Aldrich, USA).

Quantitative Real-Time PCR

Total RNA was isolated from the limb and tail tissue homogenates using TRIzol reagent (Applied Biosystems, USA). One microgram of total RNA was reverse-transcribed to cDNA using a one-step cDNA Synthesis Kit (Applied Biosystems, USA). Primers were designed using PrimerBlast tool of NCBI, details of which are given in the Appendix I. Quantitative real-time PCR was performed on a LightCycler 96 (Roche Diagnostics, Switzerland) with the following program: 3 min at 95 ºC as initial denaturation step and 45 cycles with each cycle of 10 s at 95 ºC, 30 s at 60 ºC and 30 s at 72 ºC). Gel electrophoresis and melt curve analysis were used to confirm specific product formation. 18SrRNA was taken as the endogenous control. The fold change was computed using the method of Livak and Schmittgen (Livak and Schmittgen, 2011). In order to minimize variations among biological individuals, the tissue samples from six lizards were pooled, and for each variable analysed in RT-PCR, three technical replicates were performed to reduce the experimental error.

Gelatin Zymography

Tissue collection and homogenization was done in lysis buffer containing protease inhibitor, and the tissue was homogenized at 4 °C. ABCAM protocol was followed to observe the MMP2 and MMP9 activity (Gelatin zymography protocol; Abcam. www.abcam.com). Following homogenization and centrifugation, (11,000 g for 15 min at 4 °C) the supernatant

was added to the sample buffer (1.5 M Tris pH6.8, 10 % glycerol, 2 % SDS and 0.002 % bromophenol blue) and 30 µg of total protein from each sample was loaded on a 7.5 % SDS-PAGE (polyacrylamide gel electrophoresis) gel, containing 0.5 % gelatin and allowed to run at 4 °C at constant voltage (100 V). Following electrophoresis, gels were washed with Triton wash buffer (20 mM Tris pH8, 0.15 M NaCl, 5mM $CaCl_2$, 2.5 % Triton X-100) and then incubated in incubation buffer (50 mM Tris pH7.5, 0.2 M NaCl, 5mM $CaCl_2$, 0.02 % NaN_3, 0.02 % Brij35 2.5 % Triton X-100) overnight at 37 °C for re-activation of the MMPs. Gels were stained with 0.5 % Coomassie brilliant blue R-250, where bands appeared as clear area against the dark blue background of stained gelatin. Relative intensities were determined using Doc-ItLs software (GeNei, Merck; www.merck.com).

Statistical analysis

The data presented in the current study was subjected to one-way ANOVA followed by Bonferroni post-hoc test for multiple group comparison using GraphPad Prism software Version 7 (GraphPad Software, Inc., San Diego, CA). A 'p' value of 0.05 or less was considered as being statistically significant.

RESULTS

Analysis of the transcripts of the genes involved in the process of epithelial to mesenchymal transitions

For this study, the genes targeted were *ecadherin*, *ncadherin*, *vimentin*, *mmp2*, *mmp9*, *timp2*, *timp3*, *twist1*, and *snail2*.

During the wound healing stages of tail, it was observed that the levels of *ecadherin* were significantly high at 1 dpa ($p \leq 0.001$), however, a slight decline was observed at 3 dpa ($p \leq 0.05$). After 3 dpa a sharp regression in the levels was observed until 6 dpa (Table 5.1 and Figure 5.2 A). On the other hand, the amputated limb showed heightened expression ($p \leq 0.001$) of *ecadherin* at all the selected time points viz., 6 dpa, 9 dpa, and 12 dpa indicating the resting nature of epithelial cells present at the wound site (Table 5.2; Figure 5.2 B). However, the expression of *ncadherin*, which is a marker for mesenchymal cells, showed a steady increase in the healing tail starting 1 dpa and the maximum expression was recorded at 6 dpa ($p \leq 0.001$) (which is the blastema stage of regeneration) (Table 5.1; Figure 5.2 C). However, level of *ncadherin* remained low all through the selected duration of experiment in the

healing limb indicating the absence of mesenchymal cell population therein ($p \leq 0.001$) (Table 5.2; Figure 5.2 D). Another marker for mesenchymal cell, namely, *vimentin*, indicated a similar trend as that of *ncadherin* transcript. The tail from 1 dpa till 6 dpa exhibited a steady but significant increase in the levels of vimentin ($p \leq 0.001$) (Table 5.1; Figure 5.2 E), whereas the same was not observed in the limb as the levels were drastically reduced (Table 5.2; Figure 5.2 F).

Apart from the genes expressed by epithelial and mesenchymal cells, other genes that facilitate EMT were also studied. The first to study was the expression of *mmp2* and *mmp9*, two well known gelatinases, which digest the extracellular matrix (ECM) and hence aid the EMT process. The results indicated, a 4-fold increase in the *mmp2* levels till 4 dpa ($p \leq 0.05$) in lizards' tail, which increased even further by 10-fold at 6 dpa ($p \leq 0.001$) (Table 5.3; Figure 5.3 A). During the healing stages of limb, *mmp2* levels were found lowered for all the three selected time points (6 dpa, 9 dpa, and 12 dpa) ($p \leq 0.05$) (Table 5.4; Figure 5.3 B). The *mmp9* showed similar results in the autotomised tail as was the case of *mmp2*, however, rather than showing a sharp increase at 6 dpa, *mmp9* levels started rising up from 4 dpa itself ($p \leq 0.001$) (Table 5.3; Figure 5.3 C). A slight but non-significant rise of *mmp9* levels was observed in the healing limb at 6 dpa and 9 dpa however, at 12 dpa significant downregulation ($p \leq 0.001$) of this transcript was evident (Table 5.4; Figure 5.3 D).

Parallelly, the inhibitors of *mmp2* and *mmp9* namely *timp2* and *timp3* were also assessed at mRNA level. Both *timp2* and *timp3* were found downregulated from 1 dpa till 6 dpa ($p \leq 0.001$) in the healing tail (Table 5.3 and Figure 5.4 A and C). However, the healing limb showed a different trend of transcript levels, wherein *timp2* levels remain unchanged till 6 dpa, whereas at 9 dpa and 12 dpa a significant increase ($p \leq 0.001$) was observed (Table 5.4 and Figure 5.4 B). Nonetheless, *timp3* levels were seen to be elevated from 6 dpa to 9 dpa, and maintained the high level even at 12 dpa (Table 5.4 and Figure 5.4 D).

Additionally, the mRNA levels of *snail2* and *twist1,* which are the key regulators of EMT, were reviewed. The healing tail showed promising levels of *snail2* and *twist1* at 4 dpa ($p \leq 0.01$) and 6 dpa ($p \leq 0.001$). However, no significant difference was evident during the initial phases (1 dpa till 3 dpa) of healing in case of tail. (Table 5.1; Figure 5.5 A and C). Nonetheless, the healing limb showed no increase in transcript levels of either *snail2* or

twist1 during any of the selected wound healing stages, instead, at 9 dpa and 12 dpa, their levels declined significantly ($p \leq 0.001$) (Table 5.2; Figure 5.5 B and D).

Western blot analysis of proteins involved in the process of epithelial to mesenchymal transitions

In order to reaffirm the results of the transcript level analysis, the expression pattern of certain selected protein like E-Cadherin, N-Cadherin, Vimentin, MMP2, and MMP9 were studied by carrying out western blot. The blots acquired for tail at 0 dpa, 3dpa, 4 dpa and 6 dpa revealed no change in the levels of E-Cadherin (Table 5.7; Figure 5.6) whereas, in limb, after 0 dpa all the time point showed increase ($p \leq 0.001$) in the level of protein when compared to that of resting stage (Table 5.7; Figure 5.7). N-Cadherin when assessed showed marginal increase in its levels in the healing tail starting from 0 dpa till 3 dpa ($p \leq 0.01$) however, highly significant increase was observed from 3 dpa until 6 dpa ($p \leq 0.001$) (Table 5.7; Figure 5.6). However, healing limb showed little or no change in N-Cadherin levels at any of the selected stages when compared to the resting limb (0 dpa) (Table 5.8; Figure 5.7). Vimentin showed an increase in protein level from 4 dpa and kept increasing until 6 dpa in the healing tail ($p \leq 0.001$) (Table 5.7; Figure 5.6). On the other hand, healing limb showed a hike in vimentin level only at 12 dpa ($p \leq 0.01$), otherwise, in all the other time points no significant change was noticed in the protein level when compared with the resting stage, i.e. 0 dpa limb (Table 5.8; Figure 5.7). After assessing the cell adhesion molecules, the level of MMPs was measured. In the tail, MMP2 expression was evident from the beginning itself, which is from 3 dpa onwards and the levels remained high till 6 dpa ($p \leq 0.001$). However, MMP9 increased only after 3 dpa, i.e., from 4 dpa and kept increasing till 6 dpa ($p \leq 0.001$) (Table 5.7; Figure 5.6). Contrastingly, during the limb healing process, MMP2 levels did not show any significant difference when compared to the resting limb. Nonetheless, MMP9 did show a slight but significant increase at 6 dpa and at 9 dpa ($p \leq 0.001$) but these levels subdued at 12 dpa (Table 5.8; Figure 5.7).

Transcript and protein level expression of FGF

After analysing the expression levels of genes involved in the process of EMT, fgfs were screened at transcript level. The results revealed that levels of *fgf2* and *fgf8* remained consistently high during the selected stages of healing tail i.e. from 1 dpa to 6 dpa ($p \leq 0.001$) (Table 5.5, Figure 5.8 A, and C). However, *fgf4* levels did not show any significant increase

in the earlier phase of healing, a hike in its level was seen only after 4 dpa and further increase was noted at 6 dpa ($p \leq 0.001$) (Table 5.5, Figure 5.8 B). *Fgf19* was initially found lowered in tail at 1 dpa ($p \leq 0.001$) but then a slight but insignificant rise was noted at 3 dpa, and then slowly an increase in the transcripts was seen from 4 dpa, and it peaked at 6 dpa ($p \leq 0.001$) (Table 5.5, Figure 5.8 D). Nonetheless, the healing limb had a completely different fgf expression trend, showing no change in *fgf2* and *fgf8* levels initially till 6 dpa, but a decrease was observed at 9 dpa ($p \leq 0.01$). This decrease in *fgf2* and *fgf8* levels were maintained, and hence at 12 dpa also the levels remained significantly ($p \leq 0.001$) low in the healing tissues of limb (Table 5.6, Figure 5.9 A, and C). Further it was noticed that *Fgf4* levels remain unaltered in the limb throughout the wound healing process when compared to the resting stage (0 dpa) (Table 5.6, Figure 5.9 B). The *Fgf 19* levels in the healing limb showed no change at 6 dpa, but a significant ($p \leq 0.05$) increase in its level was observed at 9 and 12 dpa (Table 5.6, Figure 5.9 D). FGF2 western blot confirmed the results obtained from gene expression analysis. In tail, a steady increase in FGF2 was observed from 0dpa to 4 dpa. However 6 dpa depicted maximum protein level ($p \leq 0.001$) (Table 5.7, Figure 5.6). Contrastingly, FGF2 levels never changed in the healing limb when compared to 0 dpa albeit a slight increase at 6 dpa (Table 5.8, Figure 5.7).

Immunohistochemical localization of E-Cadherin and N-Cadherin in the healing tail and limb

E-Cadherin and N-Cadherin were localized in the tail tissues at 0, 1, 3, 4, and 6 dpa while for the limb, the stages chosen were 0, 6, 9, and 12 dpa. The microscopic analysis revealed the presence of E-Cadherin in the epidermis of the resting tail tissue (0 dpa), but following amputation at 1 dpa no expression was observed at the wound site (Table 5.9, Figure 5.10 A and B). However, after three days of autotomy (3 dpa) in the tail tissue E-Cadherin protein was seen just near the AEC (Table 5.9, Figure 5.10 C). Subsequently, at 4 dpa and 6 dpa also no change in the position of the protein was noticed in tail and E-Cadherin remained localized in few cell layers of AEC (Table 5.9, Figure 5.10 D, and E). When E-Cadherin was localized in resting limb and in the healing stages post-amputation, the epidermis was positively stained at 0 dpa, but no sign of expression was visible at the injury site (Table 5.10, Figure 5.11 A). However, at 6 dpa faint positive signal was seen in the limb tissue at the wound site but proper localization in the epidermis covering the wound was visible at 9 dpa and more intense signal was seen at 12 dpa. Interestingly, as compared to tail at 6 dpa, the expression of E-Cadherin was seen more profusely in the wound site of limb at 9 and 12 dpa

(Table 5.10, Figure 5.11B, C and D). In tandem with E-Cadherin, the site of N-Cadherin, a marker of mesenchymal cells was studied in both the healing appendages of lizard. In the tail, we observed that at 0 and 1 dpa no protein was visible (Table 5.9, Figure 5.12 A and B), however, from 3 dpa till 6 dpa, N-Cadherin was localized in the mesenchyme close to AEC (Table 5.9, Figure 5.12 C, D and E). The cells expressing N-Cadherin kept increasing from 3 dpa to 4 dpa with maximum intensity observed at 6 dpa. In case of limb, 0 dpa and 6 dpa showed no signs of N-Cadherin protein expressing cells (Table 5.10, Figure 5.13 A and B), however between the epidermis and the scarred tissue, few cells showed positive staining at 9 dpa (Table 5.10, Figure 5.13 C). Nonetheless, this expression was short-lived, and at 12 dpa no signs of the protein were visible in the limb tissue (Table 5.10, Figure 5.13 D). The expression of the protein was quantified using ImageJ software, and the values have been depicted in Table 5.9 and 5.10.

Gelatin Zymography

For measuring the activity of MMP2 and MMP9, gelatin zymography was performed as mentioned, in the materials and methods section. The zymogram of the protein samples harvested from various stages of healing tail revealed a steady increase in the activity of active MMP2 from 1 dpa till 4 dpa and then remained constant at 6 dpa. The activity levels of MMP9 showed upward trend from 3 dpa till 6 dpa with the highest activity at 6 dpa, suggesting most ECM remodelling occurring during blastema formation (Figure 5.14 A). The activity of MMP2 in the limb healing stages showed a different trend than that observed in the tail, wherein a marginal activity was observed at 6 dpa and 9 dpa, but 0 and 12 dpa showed no signs of activity. The activity of MMP9, on the other hand, increased only during 9 dpa and all the other stages showed similar activity as that of 0 dpa limb (Figure 5.14 B).

Table 5.1: Relative gene expression data of *ecadherin*, *ncadherin* and *vimentin* observed during the healing tail

	Fold change (Mean ± SEM)			
Gene Name	**1 dpa**	**3dpa**	**4dpa**	**6 dpa**
ecadherin	$5.56 \pm 0.8^{***}$	$2.6 \pm 0.28^{*}$	1.5 ± 0.08	1.2 ± 0.001
ncadherin	$6.3 \pm 0.6^{***}$	$20.5 \pm 1.32^{***}$	$22.21 \pm 2.24^{***}$	$38.67 \pm 2.43^{***}$
vimentin	$5.5 \pm 0.52^{**}$	$9.62 \pm 0.91^{***}$	$12.56 \pm 1.3^{***}$	$20.12 \pm 2^{***}$
snail2	1.3 ± 0.29	1.9 ± 0.56	$6.37 \pm 0.41^{**}$	$8.9 \pm 0.94^{***}$
twist1	1.1 ± 0.034	1.67 ± 0.05	$6.39 \pm 0.45^{**}$	$9.28 \pm 0.61^{***}$

The given values are expressed as Mean ± SEM, * $p \leq 0.05$, ** $p \leq 0.01$ and *** $p \leq 0.001$ (n=6).

Table 5.2: Relative gene expression data of *ecadherin*, *ncadherin* and *vimentin* during observed during the healing limb

	Fold change (Mean ± SEM)		
Gene Name	**6 dpa**	**9 dpa**	**12 dpa**
ecadherin	$14.97 \pm 1.46^{***}$	$13.25 \pm 1.34^{***}$	$13.24 \pm 1.3^{***}$
ncadherin	$0.48 \pm 0.046^{*}$	$0.25 \pm 0.026^{**}$	$0.083 \pm 0.008^{***}$
vimentin	$0.35 \pm 0.034^{*}$	$0.125 \pm 0.013^{**}$	$0.0756 \pm 0.0076^{***}$
snail2	0.6 ± 0.03	$0.07 \pm 0.0032^{***}$	$0.04 \pm 0.0032^{***}$
twist1	0.69 ± 0.045	$0.04 \pm 0.0062^{***}$	$0.05 \pm 0.0023^{***}$

The given values are expressed as Mean ± SEM, * $p \leq 0.05$, ** $p \leq 0.01$ and *** $p \leq 0.001$ (n=6).

Table 5.3: Relative gene expression data of *mmp2, mmp9, timp2* and *timp3* observed during the healing tail

	Fold change (Mean ± SEM)			
Gene Name	**1 dpa**	**3 dpa**	**4 dpa**	**6 dpa**
mmp2	$3.56 \pm 0.36^{*}$	$3.66 \pm 0.34^{*}$	$3.68 \pm 0.35^{*}$	$11.23 \pm 1.11^{***}$
mmp9	$3.45 \pm 0.33^{*}$	$3.5 \pm 0.36^{*}$	$9.86 \pm 0.92^{***}$	$10.11 \pm 1^{***}$
timp2	$0.08 \pm 0.0067^{***}$	$0.05 \pm 0.0079^{***}$	$0.04 \pm 0.0062^{***}$	$0.009 \pm 0.0008^{***}$
timp3	$0.4 \pm 0.089^{*}$	$0.098 \pm 0.0035^{***}$	$0.05 \pm 0.0098^{***}$	$0.007 \pm 0.0006^{***}$

The given values are expressed as Mean ± SEM, * $p \leq 0.05$, and *** $p \leq 0.001$ (n=6).

Table 5.4: Relative gene expression data of *mmp2, mmp9, timp2* and *timp3* observed during the healing limb

	Fold change (Mean ± SEM)		
Gene Name	**6 dpa**	**9 dpa**	**12 dpa**
mmp2	$0.423 \pm 0.048^{*}$	$0.402 \pm 0.046^{*}$	$0.401 \pm 0.034^{*}$
mmp9	1.53 ± 0.13	1.835 ± 0.16	$0.423 \pm 0.04^{*}$
timp2	1.6 ± 0.43	$7.86 \pm 0.86^{***}$	$10.4 \pm 1.7^{***}$
timp3	$5.67 \pm 0.76^{**}$	$9.45 \pm 1.7^{***}$	$16.54 \pm 2.7^{***}$

The given values are expressed as Mean ± SEM, * $p \leq 0.05$, ** $p \leq 0.01$ and *** $p \leq 0.001$ (n=6).

Table 5.5: Relative gene expression data of *fgfs* observed during the healing tail

	Fold change (Mean ± SEM)			
Gene Name	**1 dpa**	**3 dpa**	**4 dpa**	**6 dpa**
fgf2	$2.87 \pm 0.19^{*}$	$3.82 \pm 0.0987^{*}$	$4.74 \pm 0.21^{*}$	$10.11 \pm 1^{***}$
fgf4	1.60 ± 0.47	1.9 ± 0.29	$8.39 \pm 1.4^{***}$	$16.31 \pm 2.73^{***}$
fgf8	$3.79 \pm 0.214^{*}$	$4.56 \pm 0.14^{*}$	$7 \pm 0.47^{***}$	$12.36 \pm 1.29^{***}$
fgf19	$0.05 \pm 0.0085^{***}$	0.8 ± 0.098	$3.98 \pm 0.093^{**}$	$7.29 \pm 1.36^{***}$

The given values are expressed as Mean ± SEM, * $p \leq 0.05$, and *** $p \leq 0.001$ (n=6).

Table 5.6: Relative gene expression data of *fgfs* observed during the healing limb

	Fold change (Mean ± SEM)		
Gene Name	**6 dpa**	**9 dpa**	**12 dpa**
fgf2	0.01 ± 0.00078***	0.13 ± 0.01**	0.15 ± 0.03**
fgf4	1.53 ± 0.13	1.835 ± 0.16	0.423 ± 0.08
fgf8	0.03 ± 0.0014***	1.1 ± 0.0968	0.423 ± 0.02
fgf19	1.78 ± 0.032	3.98 ± 0.94*	6.35 ± 1.17**

The given values are expressed as Mean ± SEM, * p≤ 0.05, ** p≤ 0.01 and *** p≤ 0.001 (n=6).

Table 5.7: Analysis of band intensity for various proteins in healing tail

	Fold change (Mean ± SEM)			
Protein	**0 dpa**	**3 dpa**	**4 dpa**	**6 dpa**
E-Cadherin	4.5 ± 0.09	4.7 ± 0.2	5.32 ± 0.56	3.89 ± 0.03
N-Cadherin	1.35 ± 0.09	8.83 ± 0.76*	28.98 ± 1.56***	43.4 ± 2.49***
Vimentin	3.42 ± 0.87	4.65 ± 0.43	9.32 ± 0.32**	17.32 ± 2.8***
MMP2	4.21 ± 0.43	12.32 ± 0.32**	18.67 ± 0.19***	25 ± 2.59***
MMP9	5.36 ± 0.71	10.45 ± 1.12*	17.63 ± 0.28***	23.29 ± 1.54***
FGF2	3.45 ± 0.39	18.29 ± 0.52***	25.37 ± 1.4***	29.52 ± 2.87***

The given values are expressed as Mean ± SEM, * p≤ 0.05, ** p≤ 0.01 and *** p≤ 0.001 (n=6).

Table 5.8: Analysis of band intensity for various proteins in healing limb

	Fold change (Mean ± SEM)			
Protein	**0 dpa**	**6 dpa**	**9 dpa**	**12 dpa**
E-Cadherin	2.78 ± 0.089	12.45 ± 0.26**	13.52 ± 1.51**	15.73 ± 3.85***
N-Cadherin	4.51 ± 0.034	5.32 ± 0.9	5.23 ± 0.53	5.46 ± 0.89
Vimentin	2.34 ± 0.019	3.87 ± 0.06	4.32 ± 0.076	12.6 ± 0.34**
MMP2	4.21 ± 0.032	5.34 ± 0.05	5.76 ± 0.065	4.9 ± 0.32**
MMP9	4.27 ± 0.04	15.81 ± 0.2***	15.29 ± 0.69***	5.32 ± 0.64
FGF2	5.29 ± 0.8	5.92 ± 0.09	5.65 ± 0.3	5.31 ± 0.8

The given values are expressed as Mean ± SEM, ** p≤ 0.01 and *** p≤ 0.001 (n=6).

Table 5.9: Immunohistochemistry analysis observed during the healing tail

	Intensity (AU)				
Protein	**0 dpa**	**1 dpa**	**3 dpa**	**4 dpa**	**6 dpa**
E-Cadherin	5.35 ± 0.09	-	7.32 ± 0.65	8.45 ± 1.46	7.43 ± 1.52
N-Cadherin	-	-	33.78 ± 2.31***	49.32 ± 1.2***	75.56 ± 3***

The given values are expressed as Mean ± SEM, *** $p \leq 0.001$ (n=6).

Table 5.10: Immunohistochemistry analysis observed during the healing limb

	Fold change (Mean ± SEM)			
Protein	**0 dpa**	**6 dpa**	**9 dpa**	**12 dpa**
E-Cadherin	2.53 ± 0.72	-	6.74 ± 1.76	9.34 ± 0.78*
N-Cadherin	-	-	5.32 ± 0.54***	-

The given values are expressed as Mean ± SEM, * $p \leq 0.05$ and *** $p \leq 0.001$ (n=6).

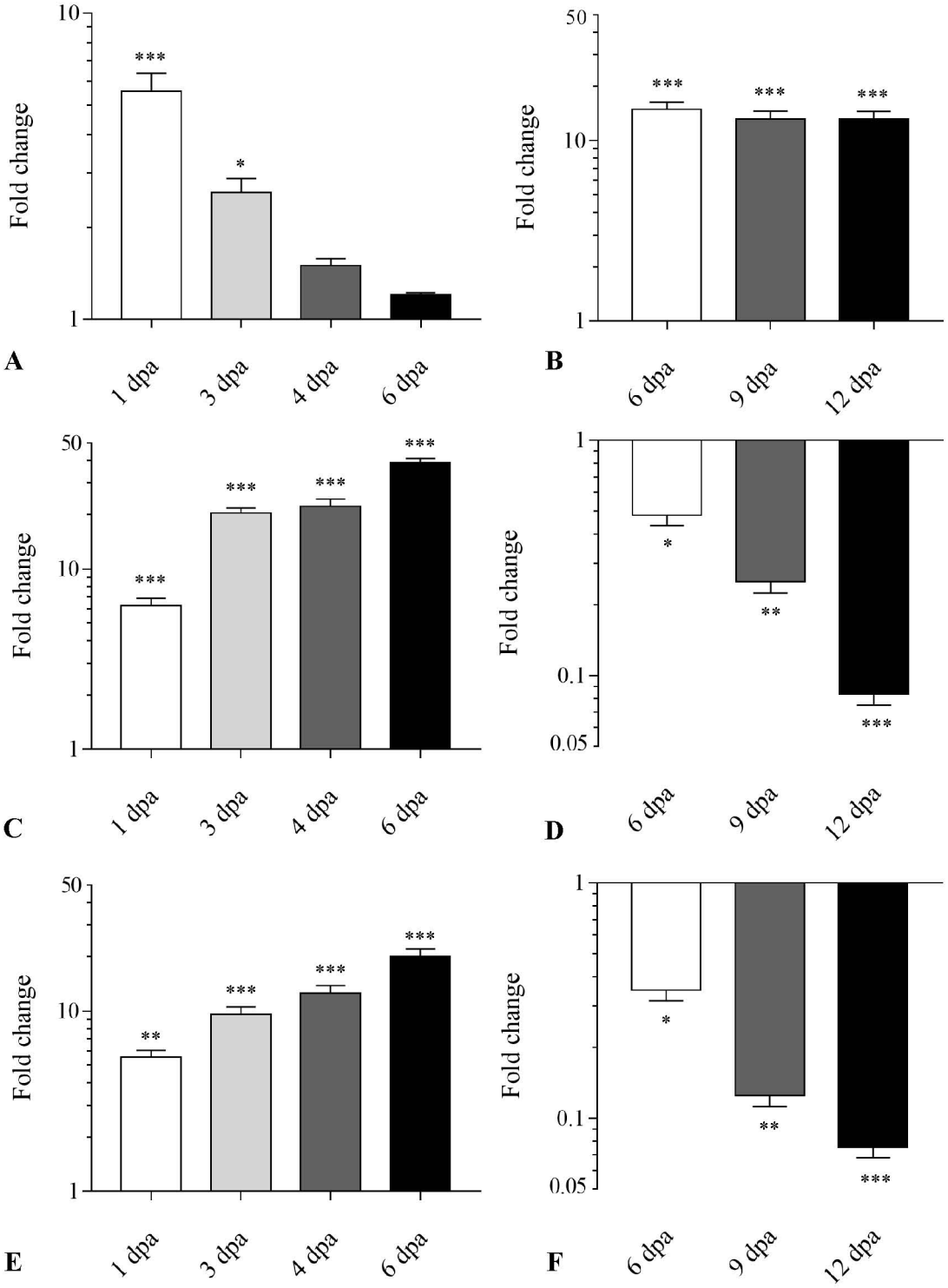

Figure 5.2: Relative gene expression for *ecadheirn*, *ncadherin* and *vimentin*

A), C) and E) Relative transcript level expression of *ecadheirn*, *ncadherin* and *vimentin* during wound healing in tail. Fold change values for time points was normalized with those of the resting stage of tail. B), D) and F) Relative transcript level expression of *ecadheirn*, *ncadherin* and *vimentin* during wound healing in the limb. Fold change values for time points was normalized with those of the resting stage of limb. Error bars represent standard error of mean and asterisk indicates p value where * shows $p \leq 0.05$, ** depicts $p \leq 0.01$ and *** stands for $p \leq 0.001$.

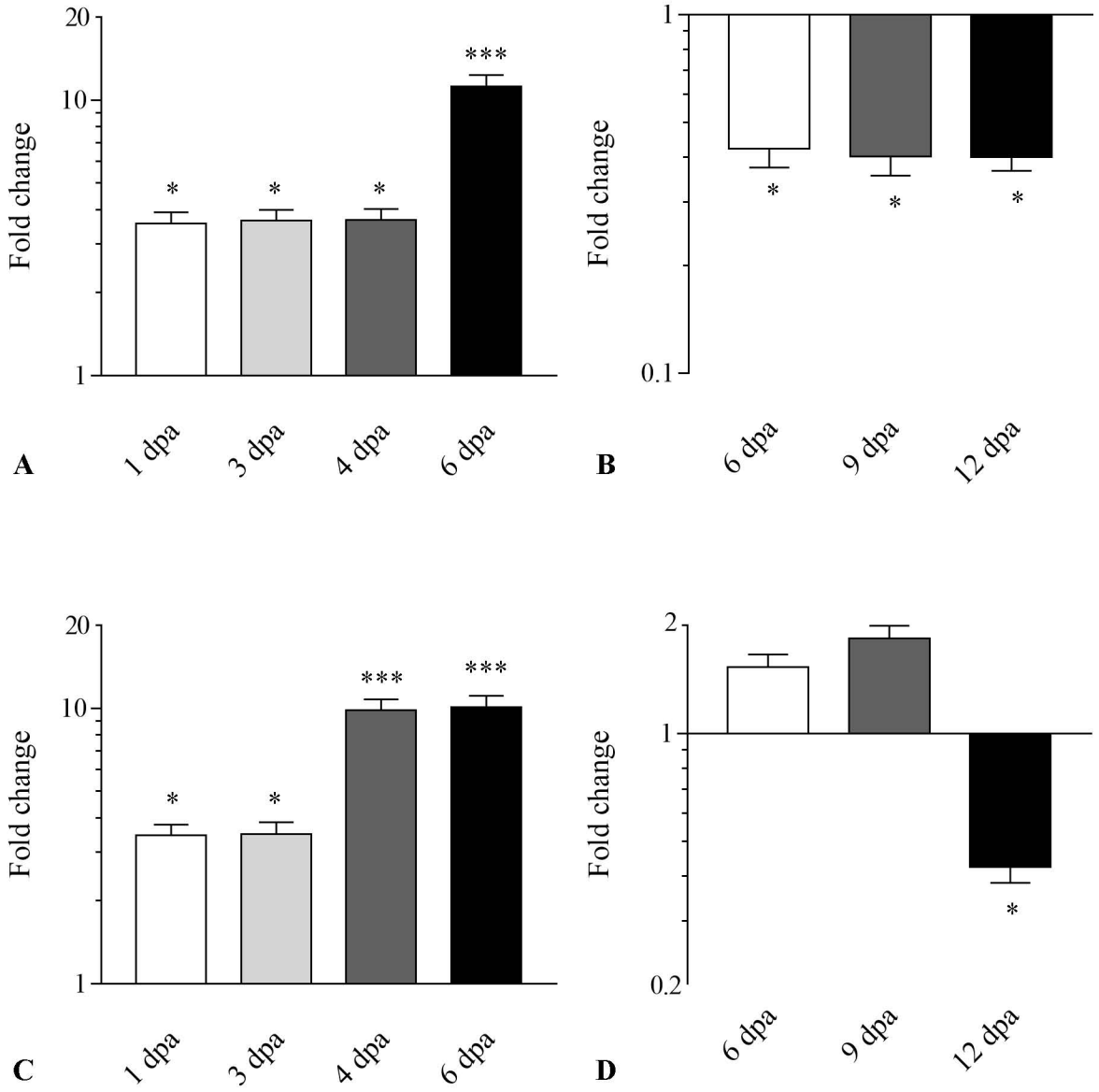

Figure 5.3: Relative gene expression for *mmp2* and *mmp9*

A) and C) show relative transcript level expression of *mmp2* and *mmp9* during wound healing in tail. Fold change values for time points was normalized with those of the resting stage of tail. B) and D) show the relative transcript level expression of *mmp2* and *mmp9* during wound healing in the limb. Fold change values for time points was normalized with those of the resting stage of limb. Error bars represent standard error of mean and asterisk indicates p value where * $p \leq 0.05$, ** $p \leq 0.01$ and *** $p \leq 0.001$.

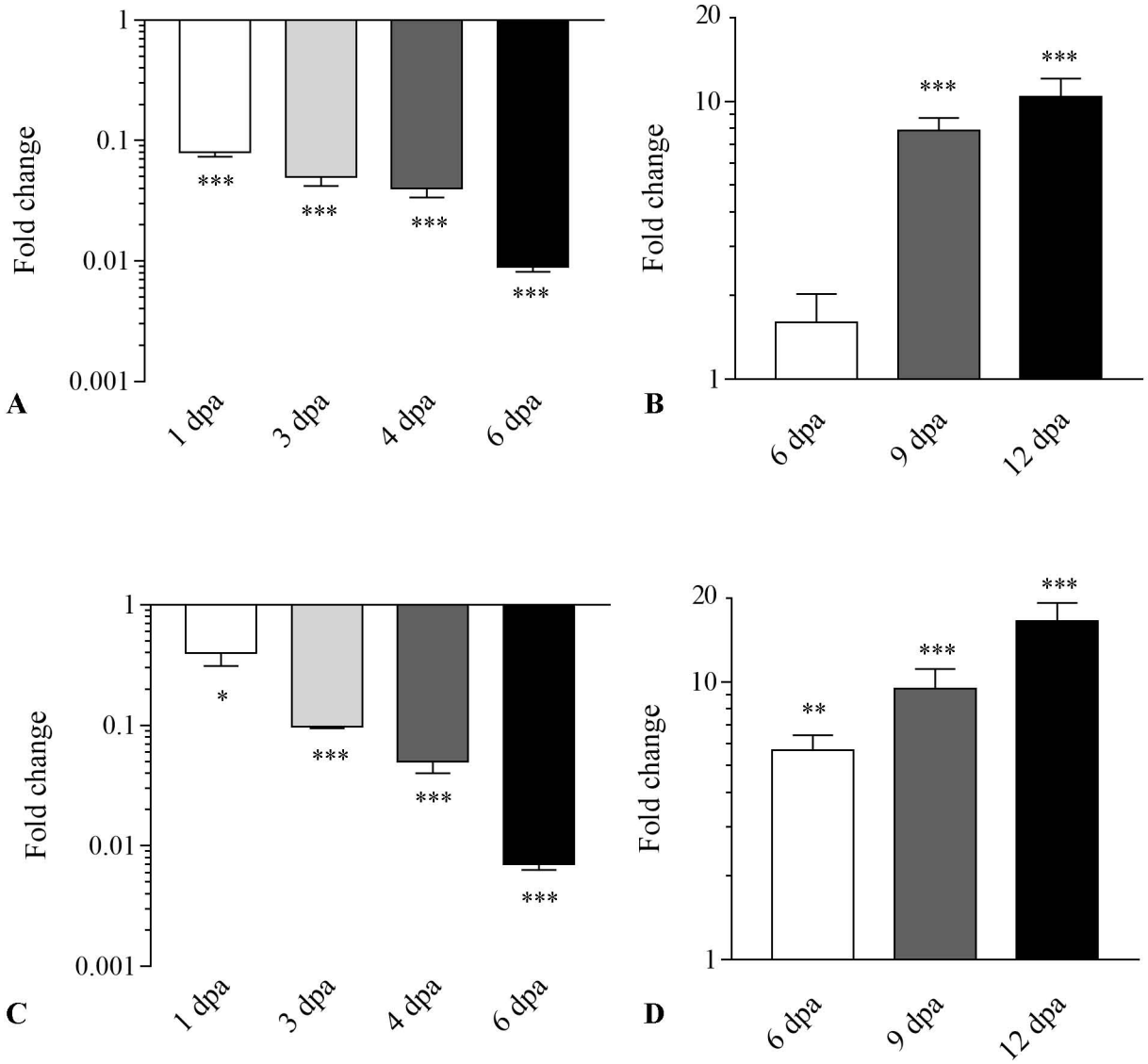

Figure 5.4: Relative gene expression for *timp2* and *timp3*

A) and C) show relative transcript level expression of *timp2* and *timp3* during wound healing in tail. Fold change values for time points was normalized with those of the resting stage of tail. B) and D) show the relative transcript level expression of *timp2* and *timp3* during wound healing in the limb. Fold change values for time points was normalized with those of the resting stage of limb. Error bars represent standard error of mean and asterisk indicates p value where * shows $p \leq 0.05$, ** depicts $p \leq 0.01$ and *** stands for $p \leq 0.001$.

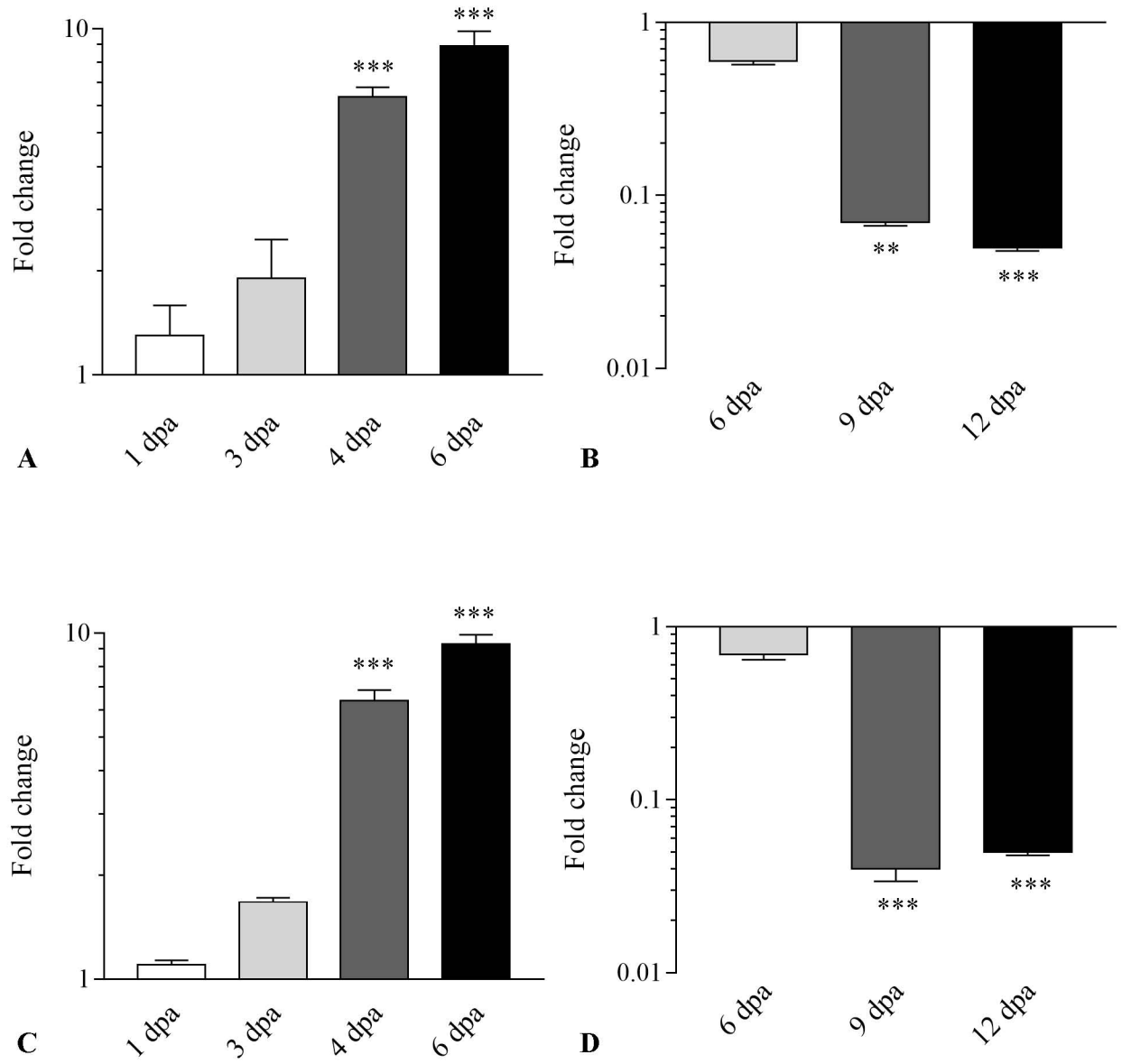

Figure 5.5: Relative gene expression for *snail2* and *twist1*

A) and C) show relative transcript level expression of *snail2* and *twist1* during wound healing in tail. Fold change values for time points was normalized with those of the resting stage of tail. B) and D) show the relative transcript level expression of *snail2* and *twist1* during wound healing in the limb. Fold change values for time points was normalized with those of the resting stage of limb. Error bars represent standard error of mean and asterisk indicates p value where * $p \leq 0.05$, ** $p \leq 0.01$ and *** $p \leq 0.001$.

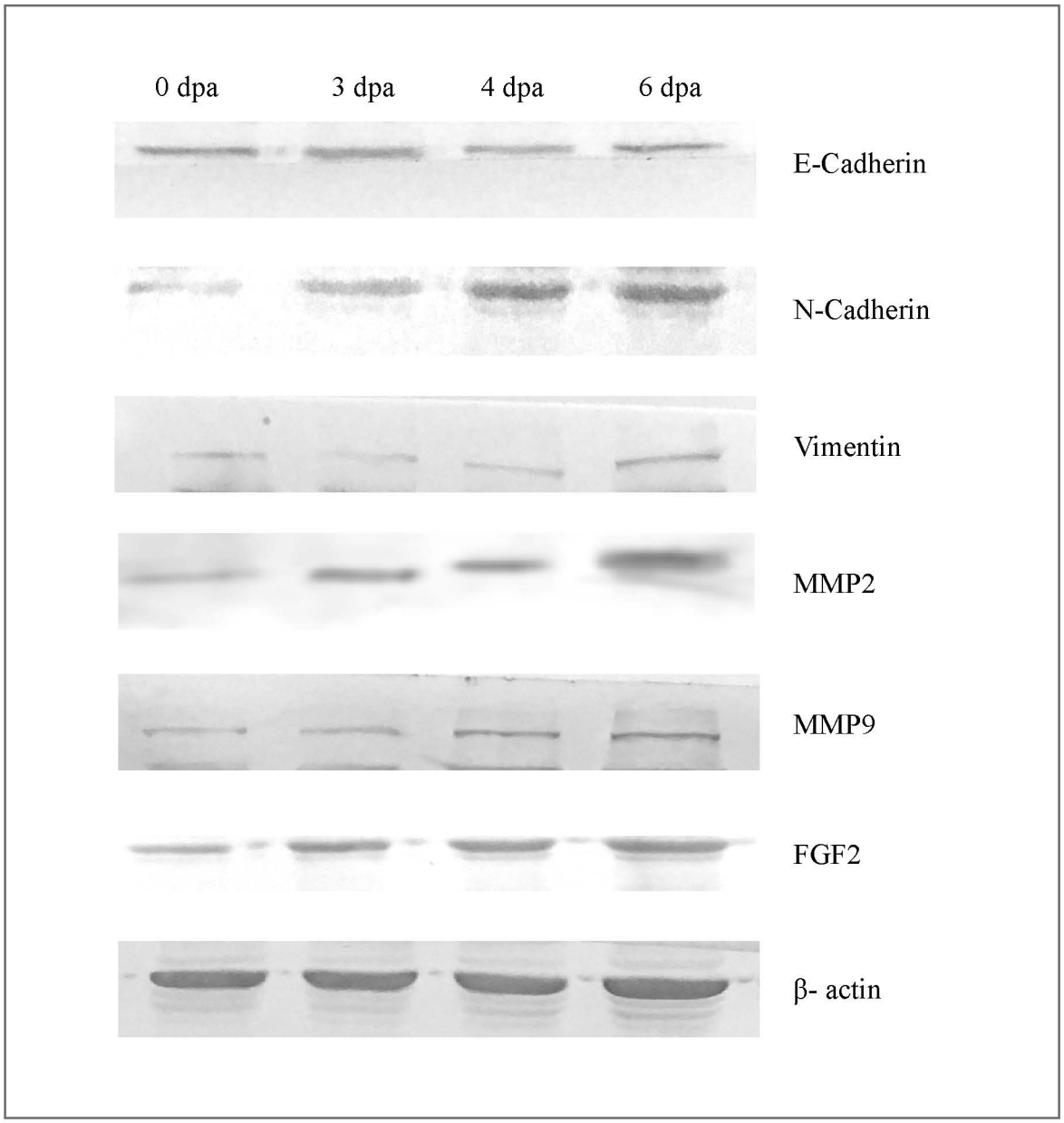

Figure 5.6: Western blot of proteins involved in the process of epithelial to mesenchymal cell transition (EMT) during tail wound healing

The proteins probed for 0, 3, 4 and 6 dpa were E-Cadherin, N-Cadherin, Vimentin, MMP2, MMP9, and FGF2. β- actin was probed for confirming the protein load. n=6.

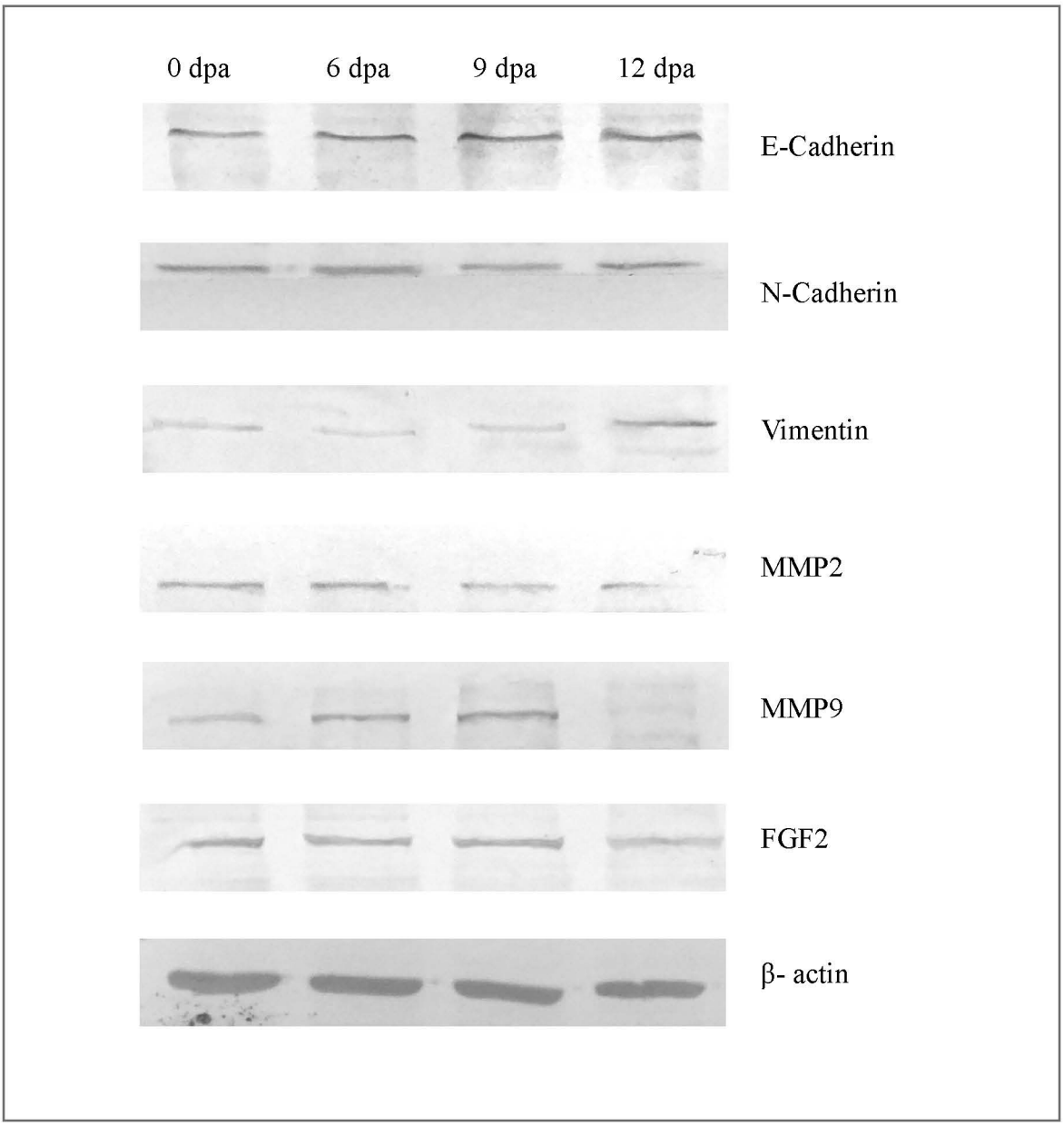

Figure 5.7: Western blot of proteins involved in the process of epithelial to mesenchymal cell transition (EMT) during limb wound healing

The proteins probed for 0, 6, 9 and 12 dpa were E-Cadherin, N-Cadherin, Vimentin, MMP2, MMP9, and FGF2. β- actin was probed for confirming the protein load. n=6.

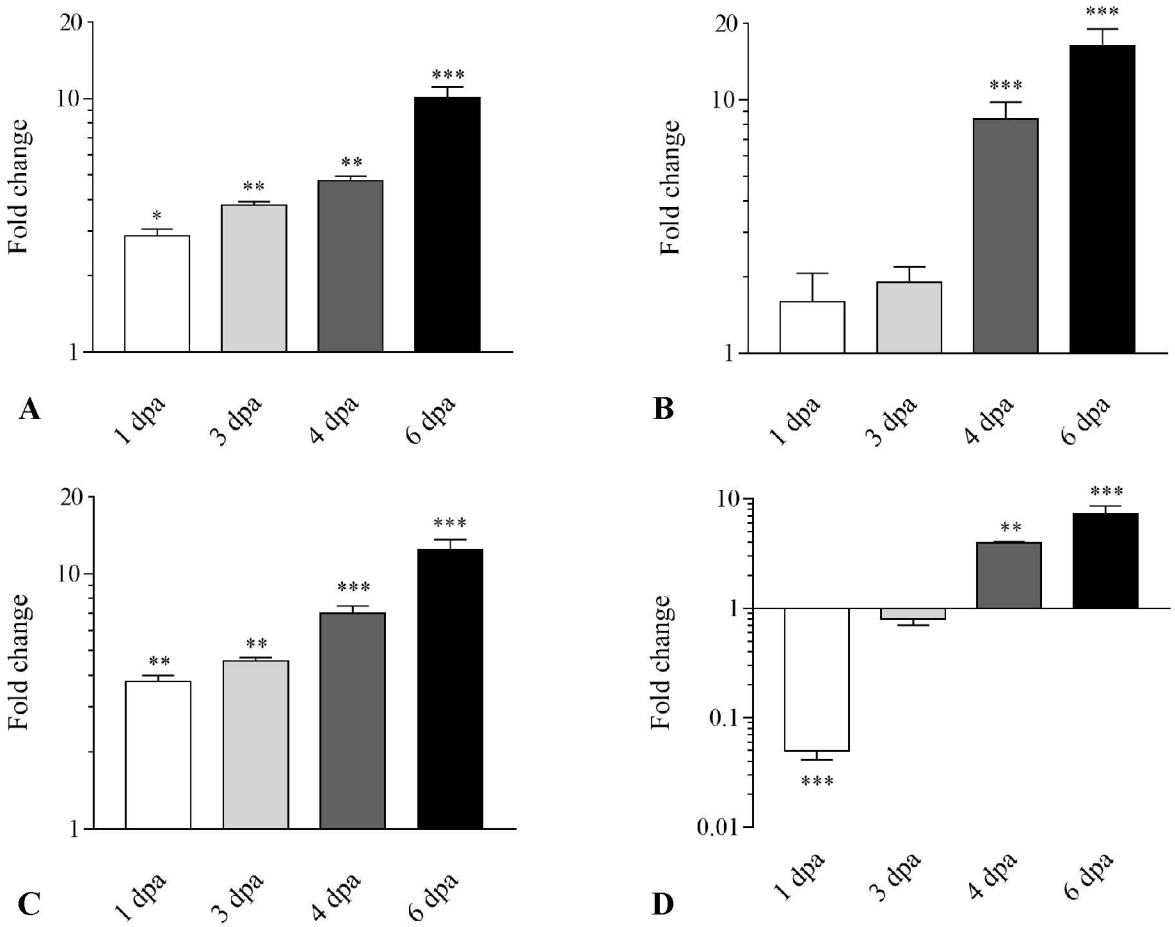

Figure 5.8: Relative gene expression for *fgfs* in tail

A), B), C) and D) depict *fgf2*, *fgf4*, *fgf8* and *fgf19* expression respectively. Fold change values for time points was normalized with those of the resting stage of tail. Error bars represent standard error of mean and asterisk indicates p value where * shows $p \leq 0.05$, ** depicts $p \leq 0.01$ and *** stands for $p \leq 0.001$.

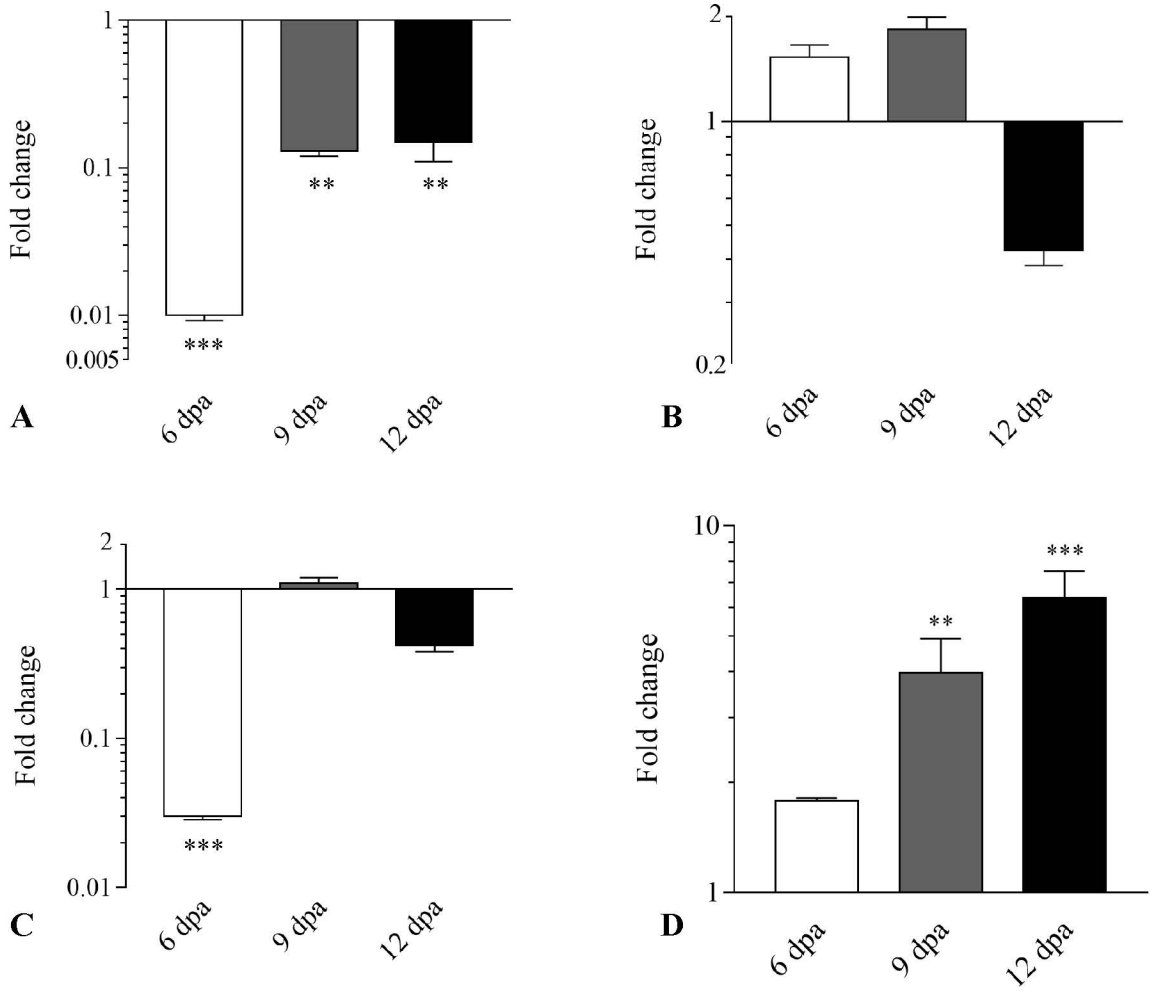

Figure 5.9: Relative gene expression for *fgfs* in limb

A), B), C) and D) depict *fgf2*, *fgf4*, *fgf8* and *fgf19* expression respectively. Fold change values for time points was normalized with those of the resting stage of limb. Error bars represent standard error of mean and asterisk indicates p value where ** depicts $p \leq 0.01$ and *** stands for $p \leq 0.001$.

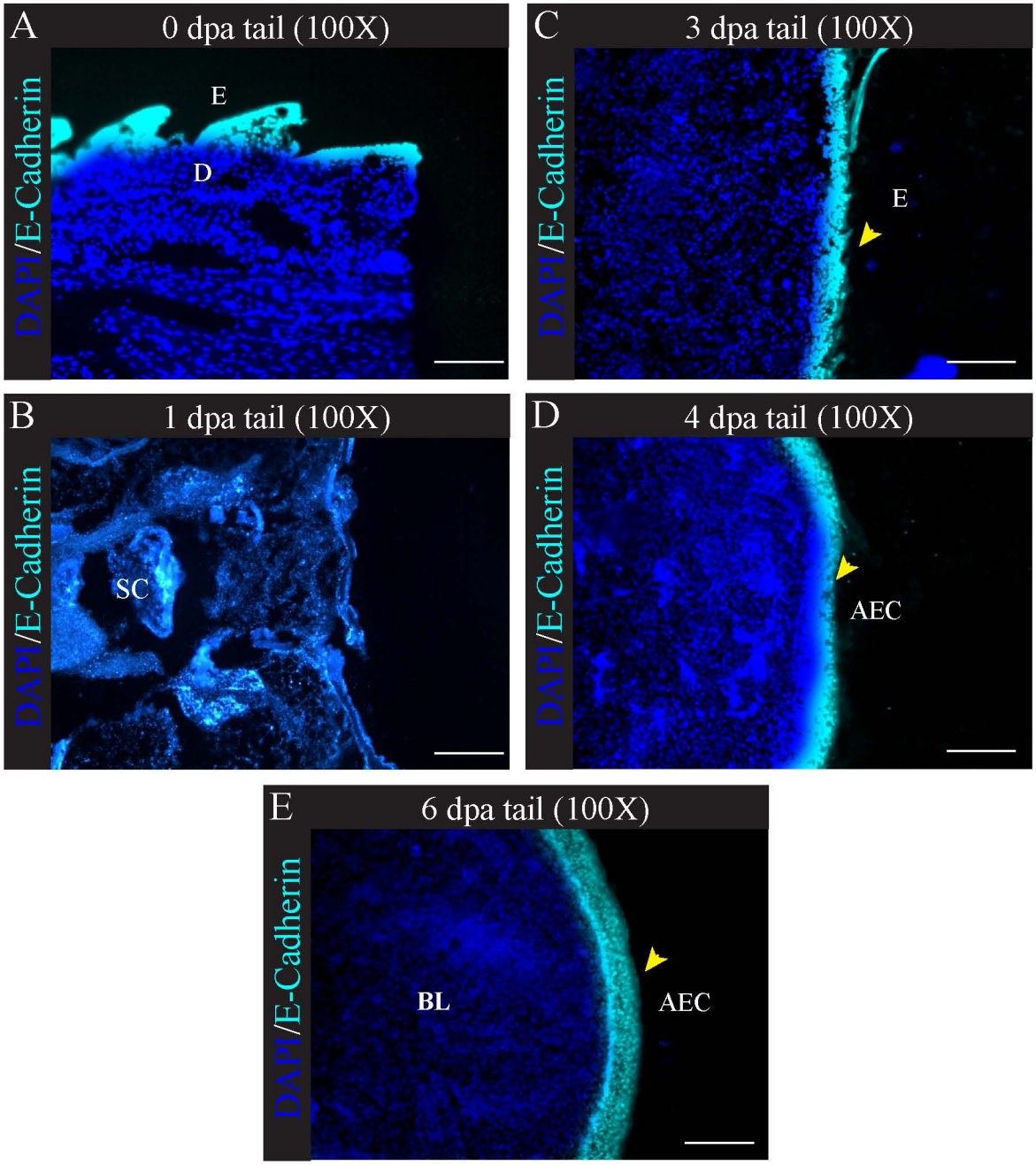

Figure 5.10: Localization of E-Cadherin in the healing tail

A) represents the 0 dpa of tail wherein the protein can be seen localized in the lateral epithelium; B) at 1 dpa no protein is visible near the wound site whereas in C) and D) which represents the 3 dpa and 4 dpa, the protein is visible only in the outer AEC. E) shows the 6 dpa which is the blastema stage wherein E-Cadherin can be observed in the outer layers of AEC. All the images are merged images wherein the cyan colour represents the E-Cadherin localized whereas the entire tissue was counter stained with DAPI. Magnification is 100X. AEC-apical epithelial cap, BL-Blastema, D-Dermis, E-Epidermis, SC-spinal cord.

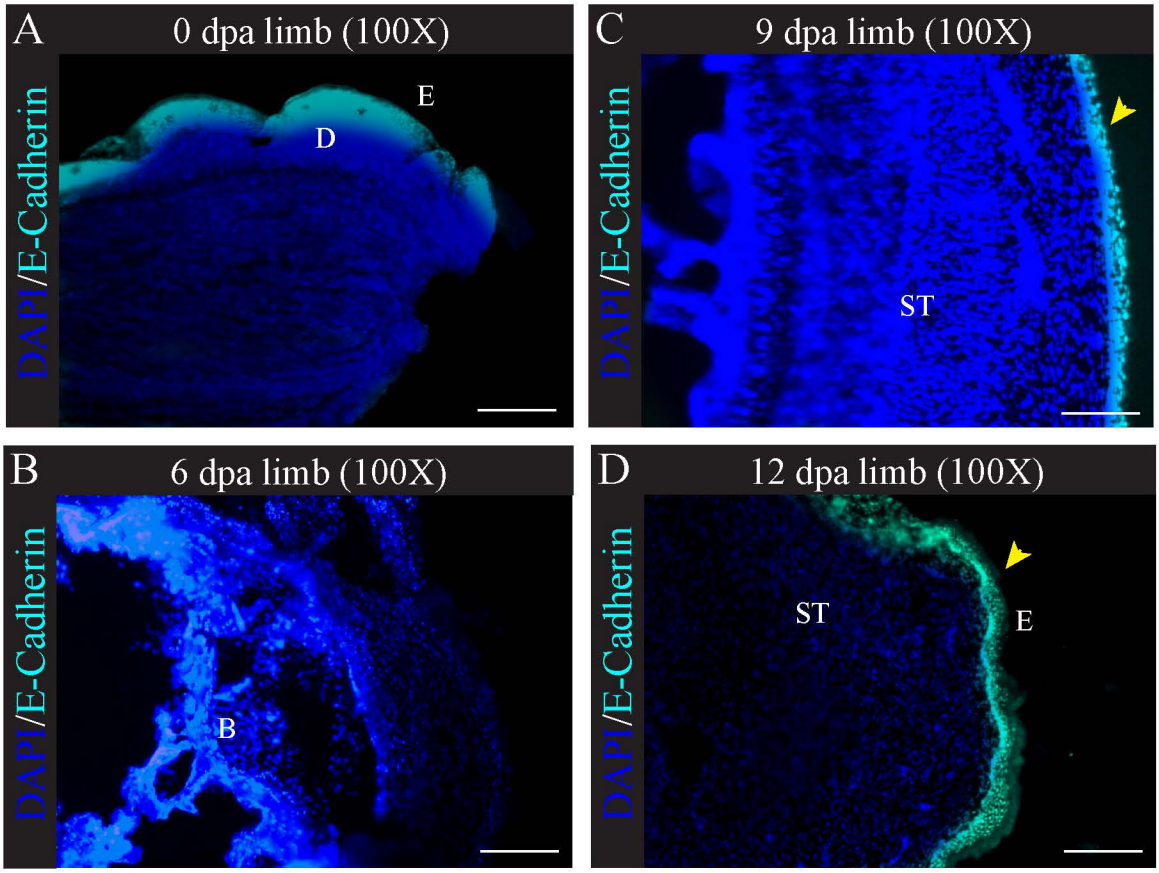

Figure 5.11: Localization of E-Cadherin in the healing limb

A) represents the 0 dpa of limb wherein the protein can be seen localized in the lateral epithelium; B) at 6 dpa no protein is visible neae the wound site whereas in C) and D) which represents the 9 dpa and 12 dpa, the protein is visible only in the outer epithelium. All the images are merged images wherein the cyan colour represents the E-Cadherin localized whereas the entire tissue was counter stained with DAPI. Magnification is 100X. B-bone, D-Dermis, E-Epidermis, ST-scar tissue

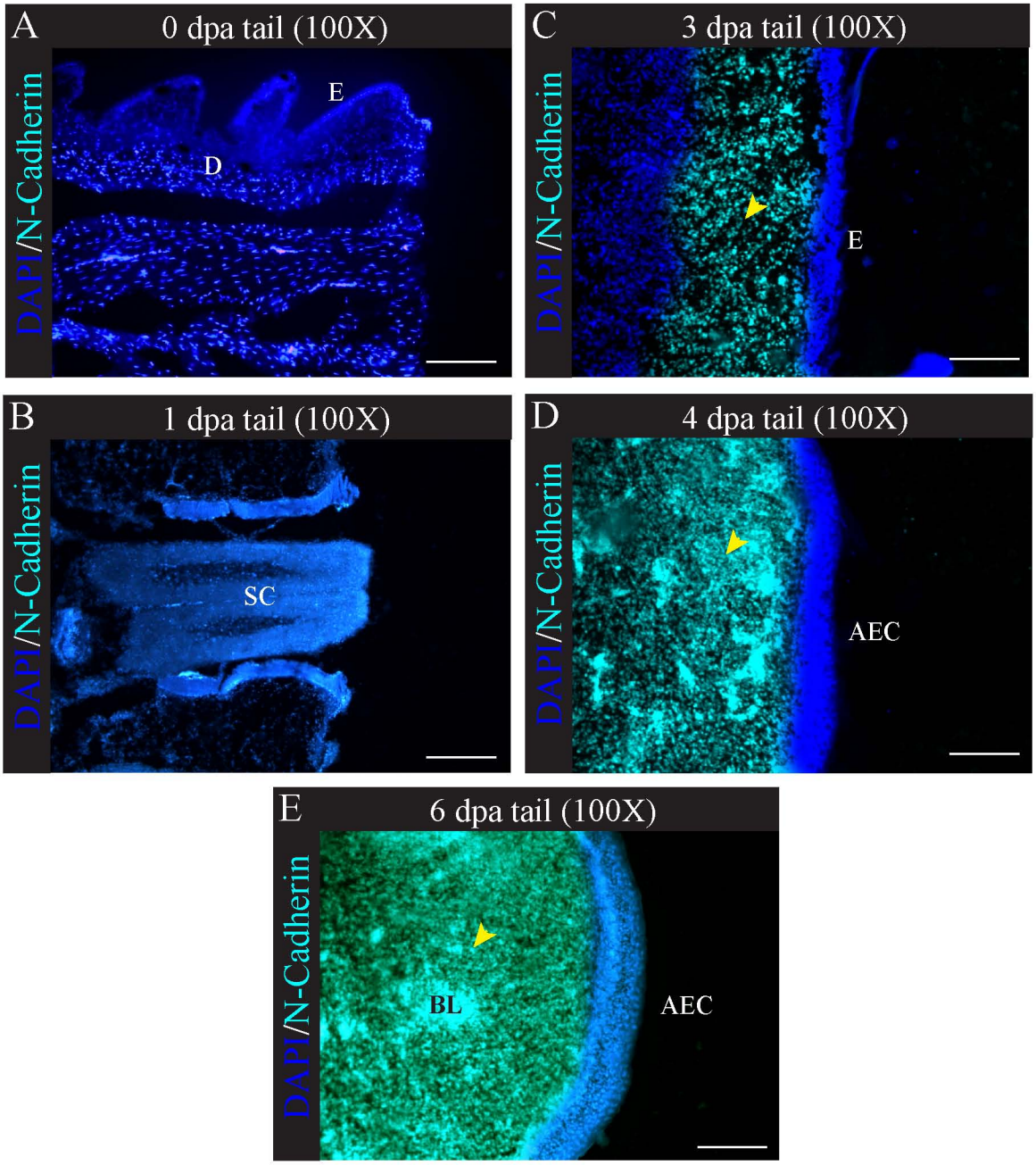

Figure 5.12: Localization of N-Cadherin in the healing tail

A) represents the 0 dpa of tail with no visible protein similarly B) even is 1 dpa N-Cadherin was absent; however an increase in protein below the AEC can be observed in C) and D) which depicts the 3 dpa and 4 dpa. E) depicts 6 dpa which is the blastema stage showing maximum N-Cadherin positive cells. The localized protein is represented by yellow arrowhead. All the images are merged images wherein the cyan colour represents the N-Cadherin localized whereas the entire tissue was counter stained with DAPI. Magnification is 100X. AEC-apical epithelial cap, BL-Blastema, D-Dermis, E-Epidermis, SC-spinal cord.

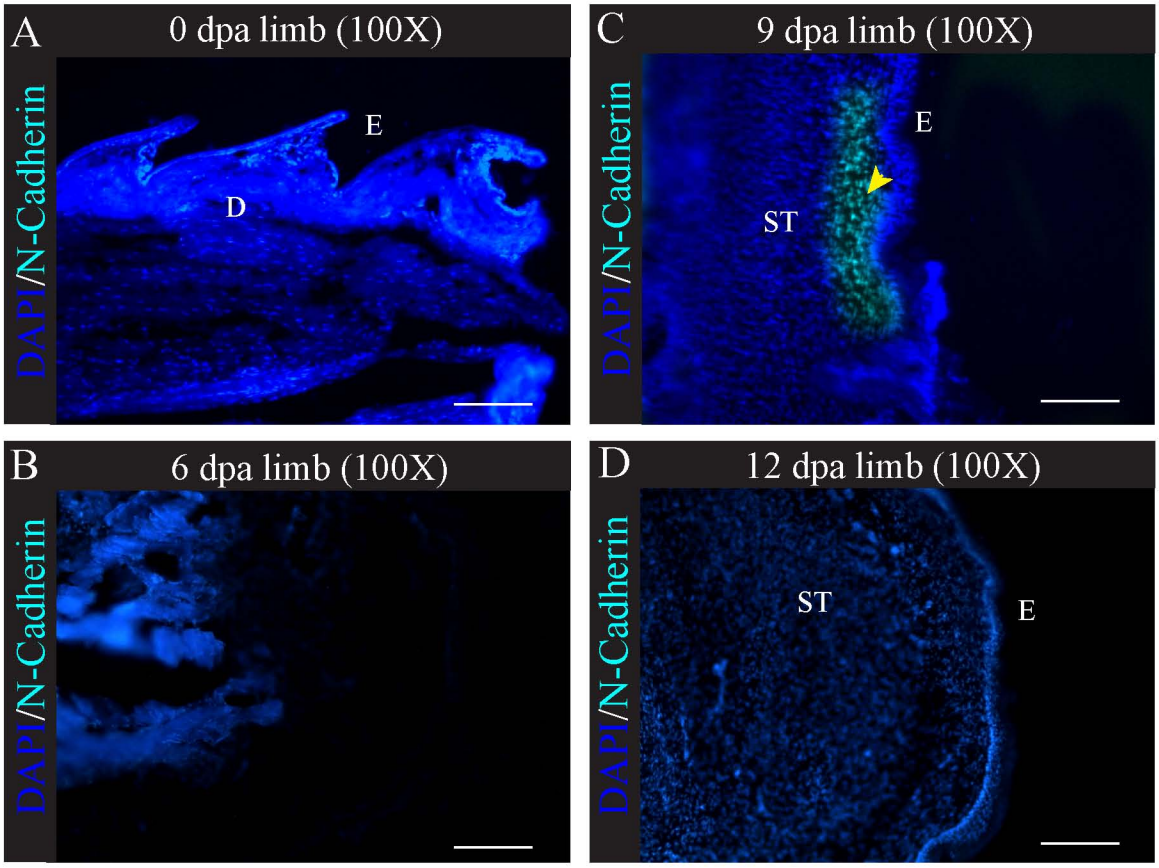

Figure 5.13: Localization of N-Cadherin in the healing limb

A) and B) represents the 0 dpa and 6 dpa of limb with no visible protein; C) 9 dpa does represent some N-Cadherin below the epidermis near the scar tissue which eventually is seen to be diminished in the D) 12 dpa image. The localized protein is represented by yellow arrowhead. All the images are merged images wherein the cyan colour represents the N-Cadherin localized whereas the entire tissue was counter stained with DAPI. Magnification is 100X. D-Dermis, E-Epidermis, ST-scar tissue.

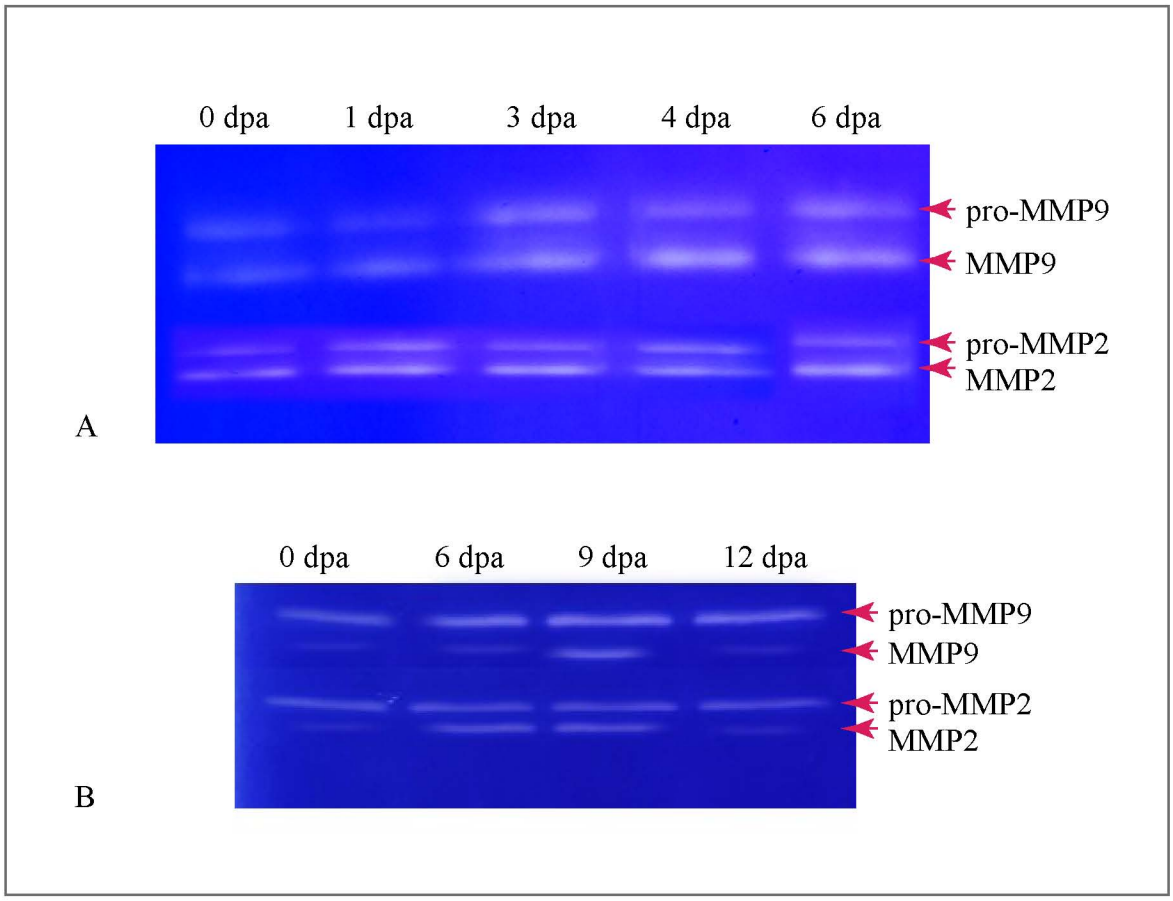

Figure 5.14: Gelatin Zymography
A) depicts the zymogram performed for tail at 0, 1, 3, 4 and 6 dpa; B) depicts the zymogram performed for limb at 0, 6, 9 and 12 dpa. The arrows indicate the bands oberved for pro-MMP9, MMP9, pro-MMP2 and MMP2 in both the gels. n=6

DISCUSSION

It is known since long that northern house geckos (*Hemidactylus flaviviridis*) can restore their lost tail all through their ontogenic development, but unfortunately they fail to develop a lost limb. Interestingly, the way in which the lizard heals its wound post-autotomy (scar-free wound healing) makes the tail regeneration compatible. The scar-free healing is achieved with the formation of a multi-layered wound epithelium viz., apical epithelial cap (AEC) at 4 dpa in *H. flaviviridis*, that trigger the formation of blastema at 6 dpa. The limb, on the other hand, cannot form this signalling centre - AEC and hence, the blastema. As mentioned in chapter 4, the proliferation of epidermal cells and the mesenchymal cells is triggered as soon as there is an injury to the tail, however, the limb shows proliferation only of the fibroblast cells at a later stage of healing. Various fgf genes were found upregulated in order to form the proliferating epidermis which eventually transforms as AEC at 4 dpa in the tail. The proliferation of epidermal cells might be a result of activation of the PI3K-Akt signalling pathway, as their levels were found to be elevated along with fgfs. Instead of proliferation at an early stage, limb showed apoptosis to be persistent for a longer duration wherein, the expression of bad and caspase 3 were seen at an early stage at 3 dpa and the latter remained high till later stages along with p53 and p21 which is triggered by the p38-MAPK pathway as evident from the result (Chapter 4). Apoptosis was apparent at 1 dpa in the tail, but it was subsequently found to be downregulated. Apart from these two processes, angiogenesis, which is the primary requirement to sustain the proliferation was also recorded in both the wound healings. In the tail, angiogenesis occurred at an early stage to provide a proliferating environment for the epidermis while, in limb at a very late stage this process was observed. Hence, VEGF-α levels were elevated throughout the process of wound healing in the tail. However, these levels shot up only at 6 dpa, which is the granulation phase in the limb, that eventually leads to scarring (Chapter 4). The current study focuses on the events which succeed the wound healing stage in tail and limb wherein proper blastema forms at around 6 dpa in the tail and in the limb no such structure is visible even after 9 dpa.

Since there are many views about the ways through which the blastemal cells arise, this study focused on the lesser explored mechanism of blastema formation, which is the epithelial to mesenchymal cell transition. Primarily, the expression of cell adhesion molecules was checked, for the EMT to occur the epithelial cells need to separate from each other in order to move (Nieto et al., 2016). The cell adhesion molecules selected were E-Cadherin, N-

cadherin, and Vimentin. E-Cadherin is known for epithelial-epithelial cell junction, which means the cells are held together when they are expressing this protein (Markiewicz et al., 2019). E-Cadherin was evaluated at both mRNA and protein levels, where the results revealed that in the tail, post-amputation no significant change was observed. Since no change in level was seen, the protein was localized at 0, 1, 3, 4 and 6 dpa and the results clearly indicate that the cells expressing E-Cadherin were present only in the outer layers of the AEC. This indicates that a proliferating AEC does not express E-Cadherin throughout, whereas, the cells towards the distal end of the tail are the only ones expressing this protein. In one of the studies performed in chick embryos, while analysing the growing hind limb bud, the E-Cadherin was localized only at the tip of the apical ectodermal ridge (AER) (Sun et al., 2002) which coincides with the current observations as AER and AEC are functionally similar. However, when E-Cadherin levels were analysed in the limb, increase in the transcripts as well as in the protein was seen, which was completely contradictory to the results obtained in the tail. There are reports that during embryonic development, cells lose cell-cell contacts, concomitantly decreasing the expression of the epithelial adherens junction molecule E-cadherin and gain expression of proteins involved in invasion and stemness (Thiery and Sleeman, 2006; Kalluri and Weinberg, 2009; Lim and Thiery, 2012). When E-Cadherin was localized in the limb at 0, 6, 9 and 12 dpa the protein was profusely localized in the entire epidermis covering the wound at 9 and 12 dpa, while 0 and 6 dpa did not show any visible expression at the wound site. The observed increase in the E-Cadherin levels could indicate that the cells are tightly attached to each other, thus leading to lowering of cell movement in the epidermis and hence, the chances of transition to mesenchymal cells are also reduced drastically. Also, in mammalian skin, the expression of E-Cadherin is found elevated during wound healing (Haensel and Dai, 2018), which matches with the expression pattern observed in wound healing stage of limb, and hence, both these structures undergo scarring. Moving further, the next molecule, which is N-Cadherin, required for the transition of epithelial cells into mesenchymal cells was studied. Our data depicts a surge in the levels of N-Cadherin during the wound healing stages of tail, i.e. from 0 dpa to 4 dpa and it hit the highest level at 6 dpa. In one of the studies in prostate cancer, when the expression of N-Cadherin was reduced, the cells could no longer have the invasive nature and hence could not metastasize (Wang et al., 2016). Moreover, it has been reported that a class switch in Cadherin i.e. form E-Cadherin to N-Cadherin, promoted EMT in breast cancer cell line MCF-10a (Park et al., 2015). Vimentin is a 57 kDa, type III intermediate filament that is found in the mesenchymal cells of various types of tissue during their developmental stages, and that

maintains cell and tissue integrity (Coulombe and Wong, 2004; Cheng and Eriksson, 2017). Intermediate filaments share common structures: the central rod domain, head domain at N-terminal and the tail domain at C-terminal (Chung et al., 2013). Switching expression types of intermediate filaments are associated with malignancy (Liu et al., 2015b). This suggests that mesenchymal cells would express Vimentin and hence, to test the hypothesis that blastemal cells do comprise of mesenchymal cells, their expression was studied. In tail, as we saw with N-Cadherin, the levels of vimentin were upregulated, however, the upregulation was observed at a later stage, i.e., from 4 dpa and not from 1 dpa. As 4 dpa marks the wound epithelium stage in the tail only after which the blastema formation starts and hence, it is possible that the expression of vimentin would commence after 4 dpa and would maximize at 6 dpa. The observed expression of vimentin in the tail goes with the hypothesis of the presence of mesenchymal cell at the blastema stage. In limb however, an increase in Vimentin was observed only at 12 dpa. Nonetheless, by 12 dpa the wound is covered with a scarred tissue and hence, even though we found some expression of the vimentin protein and transcript, blastema formation at this stage is not possible. For the blastemal cells to be maintained many paracrine factors need to come from the wound epithelium, which is not possible in a limb at 12 dpa as those factors, even if present, would not be able to cross the scarred tissue and therefore, no regeneration is possible in limb.

After analysing the levels of cell adhesion molecules in the wound healing, it was confirmed that tail during its wound healing stages does show positive results for EMT, whereas, limb does not. Furthermore, even if the cells express N-Cadherin and vimentin, it does not mean the cells would be able to move unless the extracellular matrix gets digested, and hence MMPs were looked upon along with their inhibitors, TIMPs. MMP2 and MMP9 are the gelatinases which have a primary function in digestion of the matrix in a tissue (Jabłońska-Trypuć et al., 2016; Murawala et al., 2018; Patel et al., 2019). *mmp2* gene expression depicted an increase from 1 dpa itself in the tail and remained high till 4 dpa following which at 6 dpa these levels spiked even more. This was reaffirmed by performing a western blot of MMP2 protein, and the activity was assessed by gelatin zymography. Cepeda and co-workers (2017) in their work found that MCF7 breast cancer cell line normally is not very invasive as the other cancer cell lines but when they increased the expression of MMP2, the invasive character which remained subdued initially got switched on. The cells were able to migrate efficiently, and this led to the conclusion that digestion of the matrix caused by MMP2 plays a crucial role in the cell movement. In case of healing tail of lizard, the observed increase in

the levels of MMP2 suggest that the N-Cadherin expressing cells would require the matrix digestion so that they can migrate to the boundary between the mesenchyme and the newly formed AEC. Similarly, MMP9 levels were also found upregulated in the healing tail of *H. flaviviridis*. MMP2 and MMP9 together are essential for the remodelling of ECM during development (Gawronska-Kozak et al., 2016). In the limb, however, the levels of MMP2 and MMP9 did not increase from the level observed at the resting stage (0 dpa), which does not mean that there was no activity since a basal level of activity was observed in all the healing stages of the limb. The plausible reason as to why the MMPs did not increase during wound healing of the limb may not be known, however, its implications are very clear. Since the levels did not show any rise during the early or late phases of healing, the cell movement was very restricted and hence even when N-Cadherin positive cells were present at 9 dpa of healing, they could not move and relocate to form blastema. A number of MMPs are reported to be expressed during amphibian development, which appear to be involved in the radical remodelling and cell death that occurs during amphibian metamorphosis, such as the loss of the larval tail and transformation of the intestine (Gross and Lapiere, 1962; Patterton et al., 1995; Brown et al., 1996; Ishizuya-Oka et al., 1996; Oofusa et al., 2002). The MMPs are also thought to play a role in the process of regeneration in different model systems (Yang and Bryant, 1994; Miyazaki et al., 1996; Kherif et al., 1999; Yang et al., 1999). For instance, in axolotls, MMP-9 is upregulated after limb amputation and is thought to play a role in limb regeneration (Yang and Bryant, 1994; Yang et al., 1999). It has been argued that MMPs might play a role in breaking down the ECM, which may be involved in the initial dedifferentiation of cells in preparation for regeneration and transdifferentiation (Miyazaki et al., 1996). As mentioned earlier TIMPs are the inhibitors of MMPs, their levels were also studied, and the results revealed an increase in *timp2* and *timp3* in the limb during various time points. This increase in the levels of *timps* suggests, how the levels of mmps were downregulated during the wound healing phases of limb. In chronic leg wound, the levels of mmps were reported to be subdued, while those of their inhibitors like timps were upregulated (Cook et al., 2000), suggesting how important the ECM remodelling is during the wound healing.

Although the levels of E-Cadherin, N-Cadherin, and MMPs along with *timps* were studied, one cannot be sure if the process of EMT took part in the formation of blastema during tail regeneration. Hence, two main molecules that would confirm the induction of the EMT pathway viz., snail2 and twist1 were studied herein, for their expression pattern post-

amputation/autotomy. During EMT in metastasis and in embryogenesis, many EMT-inducing transcription factors, such as Twist1, Snail1, Snail2, and ZEB2 are often found activated simultaneously in the neural crest cells (Nieto, 2002; Van de Putte et al., 2003). The analysis of the current results revealed that *snail2* and *twist1* get upregulated after 4 dpa in the lizard tail, while interestingly in the limb their levels are found lowered after 6 dpa. *Snail2* and *twist1* are known to inhibit the expression of E-Cadherin and hence in the tail, as mentioned earlier, we saw a reduction in the E-Cadherin levels, which could have been because of the increased levels of *snail2* and *twist*. Also, there are reports which mention that it is the *twist1* which activates the levels of *snail2*, which in turn leads to activation of *twist1* induced EMT (Casas et al., 2012). In tail, highest expression of these transcriptional regulators was observed at 4 and 6 dpa, and this provides some evidence pointing towards the activation of EMT during blastema formation. However, how much is the contribution of EMT towards blastema formation cannot be ascertained at this point, for which, an inhibitor against *twist* or *snail* should be used to curb the EMT and then check whether it affects overall blastema formation which nonetheless, is beyond the scope of the current study.

Notwithstanding the above described mechanisms, the EMT program is promoted by many soluble growth factors, including FGFs (Savagner et al., 1994; Katoh and Nakagama, 2014). The activation of the FGFR/ERK pathway by FGF2 normally promotes cell growth and EMT in the chordoma (Hu et al., 2014) and FGF10 can induce EMT of breast cancer cells (Abolhassani et al., 2014).It is also reported that FGF8 has the ability to induce a more aggressive phenotype displaying EMT that results in enhanced invasion and growth in colorectal cancer cells (Liu et al., 2015a). Suzuki et al. (2015) measured FGF2 expression in lung adenocarcinoma (ADC) tissues and reported high expression of the FGF2 portein is a prognostic indicator mainly for an unfavourable consequence. Donnem and colleagues while investigating non-small-cell lung cancer (NSCLC) found high expression of FGF2 and claimed that this molecule was responsible for the migration of cancerous cells (Donnem et al., 2009). In the current study, we observed an increase in the FGF2 levels both in transcript and protein, during the wound healing of the tail. This result suggests that FGF2 might have a plausible role in EMT during regeneration of lizard tail. Alternative splicing of FGFR2 mRNA generates the FGFR2-IIIb isoform, which selectively binds FGF7 with high affinity, or the FGFR2-IIIc isoform, which selectively binds FGF4. The dedicated ligands for FGFR2-IIIb and FGFR2-IIIc are usually expressed in mesenchymal and epithelial cells, respectively (Guo et al., 2012; Katoh and Nakagama, 2014). A switch from FGFR2-IIIb to FGFR2-IIIc

has been reported in the malignant progression of prostate and bladder cancer (Yan et al., 1993; Guo et al., 2012). In a study carried out Abell et al.,(2009) out of the 23 reported FGFs, they focused on FGF4 and FGF7, the representative FGF ligands for FGFR2 splice variants, and studied their functions in the EMT program of lung ADC. Experiments conducted on human lung ADC tissue samples showed that FGF4 expression was relatively high in lymph-node metastatic foci and in lung ADC tissues with metastasis. Experiments carried out on mouse, also indicated that FGF4 treatment might induce tumor metastasis. In one of their experiments when Immunohistochemical staining of human and mice tissue samples was performed, the results showed that FGF4 could actually induce an EMT phenotype. In their previous experiments also they demonstrated role of FGF4 in maintaining trophoblast stem cells under undifferentiating, self-renewing conditions. FGF4 also decreased E-cadherin expression and induced an upregulation in the levels of Slug and Twist (Abell et al., 2009). Even in the autotomised tail of lizard, a hike in *fgf4* level was evident, whereas the healing limb did not show any significant increase in its level. The present data therefore, indicate that FGF4 too plays a crucial role during EMT, and in tail, since its level peaked at 6 dpa, it can be construed that the process of EMT might have activated to initiate the process of regeneration.

Additionally, we noticed an upregulation of *fgf8* ligand during the wound healing of tail; however, in limb, *fgf8* expression was found completely diminished. As shown by Liu and co-workers (2015a), FGF8 was overexpressed in advanced colorectal cancer and according to their results, this overexpression promotes proliferation and metastasis of the cells in colorectal cancer. This is done by activating YAP1, suggesting that FGF8 helps in the process of EMT during cancer. Therefore, it is prudent to presume that the observed surge in levels of *fgf8* in lizard tail during blastema formation could be to induce the EMT process.

Furthermore, *Fgf19* levels were found upregulated in the tail after the autotomy, similarly even in the limb, heightened expression was recorded. The only difference is that in tail *fgf19* expression was found from 4 dpa while in limb it was from 9 dpa which suggests that though *fgf19* was present in limb it could not have induced EMT, since scar tissue formed by that time might acts as a barrier. Compelling evidence by Zhao and co-workers (2016b), suggests that the epithelial-mesenchymal transition correlates with aggressiveness of tumours. In cholangiocarcinoma and colorectal cancer, the process of EMT shows involvement of FGF19. However, molecular mechanisms underlying FGF19 induced EMT process remain

largely unknown in hepatocellular carcinoma. In their study, it has been shown that the expression of FGF19 was elevated significantly however inhibited the expression of E-cadherin in hepatocellular carcinoma tissues and cell lines. Moreover, it has been observed that ectopic expression of FGF19 promotes EMT and invasion in epithelial-like hepatocellular carcinoma cells through repression of E-cadherin expression (Turner and Grose, 2010), whereas FGF19 knockdown enhances E-cadherin expression.Thus diminishing EMT traits in mesenchymal-like hepatocellular carcinoma cells, which suggest that FGF19 exerts its tumour progressing functions as an EMT inducer. This finding can be correlated with our results wherein, *fgf19* levels were upregulated, and E-Cadherin was downregulated in the tail, which ultimately leads to EMT and successful regeneration subsequently.

The current study leads to a conclusion that the tail on amputation undergoes a scar-free wound healing, followed by activation of EMT pathway. The latter plays a pivotal role in blastema formation, which ultimately leads to the successful regrowth of the lost part. Limb however, did not show any signs of activation of EMT pathway. Even though, few molecules that regulate EMT showed signs of upregulation, were too late to induce EMT in limb. By the time the levels of N-Cadherin and MMPs increased, scarring had already begun failing to evoke blastema formation, resulted in the maturation of scar at the wounded site of limb.

CONCLUSION

In *Hemidactylus flaviviridis*, for the first time, we are reporting a possibility of EMT playing a crucial role during the tail regeneration. Till date, most reports were biased towards dedifferentiation of the existing cells and contribution of resident stem cells towards the blastema formation during regeneration. As EMT plays a major role during the development of most organisms, it is imperative that it would have some function during regeneration. This hypothesis of EMT participating in regeneration is based on the fact that many developmental processes do get activated during regeneration. In this study, healing stages of tail and limb were investigated to see whether there is any sign of EMT pathway getting switched on succeeding amputation and whether it affects the healing pattern. The results revealed an increase in the N-Cadherin level during the wound epithelium and blastema stage of the tail. N-Cadherin was also profusely present in the AEC and blastemal cells when localized. In limb N-Cadherin was scantily localized at 9 dpa however, by then the scarring had already initiated, and hence the cells expressing the protein would not be able to move and proliferate to make a blastema. It can be said that in tail N-Cadherin expressing cells were dominant from the early phase of wound healing when compared to the limb. E-Cadherin, on the other hand, showed no change in the levels in the tail when compared to 0 dpa. While in the limb the expression of E-Cadherin kept increasing, which does indirectly indicate the failure of the EMT. Vimentin is expressed only by the mesenchymal cells and tail showed the maximum expression of Vimentin at 6 dpa. This led us to believe that blastemal cells do have mesenchymal cells present in their vast pool of proliferating cells. To reaffirm the status of EMT activation, *snail2,* and *twist1,* which inhibit the expression of E-Cadherin and initiate the process of EMT were studied. The results revealed an increase in their levels in the tail during the healing stages whereas in the limb these levels were subdued again suggesting that this process gets activated only in the tail and not in the limb, although the reason is unknown. Though the study showed that the epithelial cells start expressing N-Cadherin by class switching and get converted to mesenchymal cells, these cells still need to move towards the underlying tissue in the blastemal zone, which is possible only when the ECM is digested. The MMP2 and MMP9, gelatinases required for ECM digestion, gave positive results in the tail. This subsequently led to a conclusion that ECM digestion occurs in the tail for tissue remodelling and for mesenchymal cell movement. We not only did a gene expression analysis by Real Time Quantitative RT-PCR but also performed a western blot and also checked the activity of MMP2 and MMP9 by gelatin zymography. Limb showed an

increase in the TIMPs, inhibitors of MMPs, which was the reason for the reduction in expression of MMPs during the healing stages. Limb overall showed no traits which could lead to activation of the EMT pathway. Additionally, *Fgf2, fgf4, fgf8, fgf19* were found to be elevated in the tail while in limb, contradictory results were obtained (Figure 5.15). FGFs have been reported to induce EMT during cancer by promoting the process of metastasis. Hence, from the results obtained, it is safe to conclude that not only during cancer but even for the regeneration of lizards tail the FGFs get activated, leading to scar-free wound healing and eventually successful regeneration.

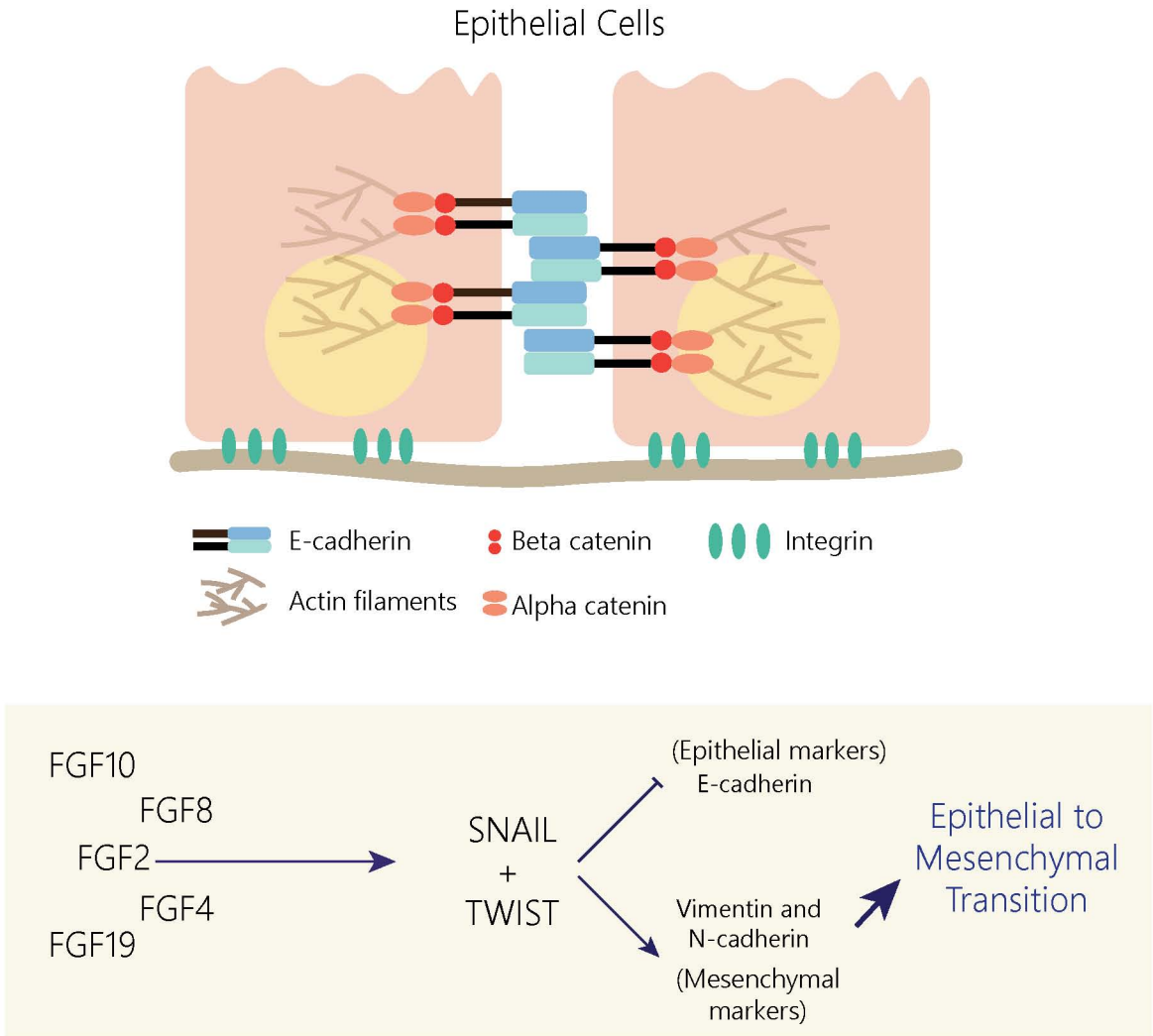

Figure 5.15: Summary of EMT process and the molecules that taking part during the healing of tail and limb